Electronic Research Archive

https://www.aimspress.com/journal/era

ERA, 34(5): 3112–3144.
DOI: 10.3934/era.2026141
Received: 12 October 2025
Revised: 13 March 2026
Accepted: 24 March 2026
Published: 09 April 2026

Research article

Dynamics and optimal control of a fractional-order plant disease model

Ismail Gad Ameen[1,*], Saud Owyed[2], Yasmeen Ahmed Gaber[1] and Hegagi Mohamed Ali[3]

[1] Department of Mathematics, Faculty of Science, Qena University, Qena 83523, Egypt

[2] Department of Mathematics, College of Science, University of Bisha, Bisha 61922, Saudi Arabia

[3] Department of Mathematics, Faculty of Science, Aswan University, Aswan 81528, Egypt

* **Correspondence:** Email: ismailgad@svu.edu.eg.

Abstract: A fractional-order model (FOM) was developed to investigate plant disease transmission (PDT) through a system of dimensionally consistent fractional differential equations (FDEs) with the Caputo derivative. The model's well-posedness was established by proving existence and uniqueness of solutions via a fixed-point theory and the contraction mapping principle. Positivity, boundedness, and the equilibrium points (EPs) of the system were then characterized, followed by an analysis of their local and global stability using the Routh-Hurwitz criteria and LaSalle's invariance principle. The control reproduction number (R_c) was derived using the next-generation matrix method, and a sensitivity analysis highlighted the parameters most influential to disease spread. A fractional optimal control problem (FOCP) incorporating preventive and curative time-dependent interventions was formulated, and necessary optimality conditions (NOCs) were obtained through a kind of Pontryagin's maximum principle (PMP). The resulting optimality system was solved numerically using a forward-backward sweep method (FBSM) based on the fractional Euler scheme, enabling the evaluation of control strategies. Three optimal intervention strategies emerged, each shaping the epidemic trajectory differently depending on the distinguishing parameter ε in the two-stage transmission process. Numerical simulations depicted the behavior of R_c across different ε and fractional order α, while tabulated objective functional values exhibited the efficacy of the proposed controls. Overall, the framework offered practical insights for mitigating and potentially eliminating plant epidemics under diverse control strategies.

Keywords: plant-disease dynamics; mathematical models; fractional optimal control problems; stability analysis; numerical simulation

1. Introduction

Plant disease epidemiology systematically studies the evolution and determinants of plant diseases within populations over time. Overall, the epidemiology of plant diseases plays a critical role in maintaining global food security [1, 2] by providing a scientific basis for developing strategies to reduce the transmission of such diseases in plants. Plants use natural immunity to defend against pests, pathogens, and insects [3, 4]. Other strategies used by farmers to prevent crop losses caused by plant epidemics include pruning and replanting. This approach offers several benefits: it eliminates diseased plants, reduces the spread of infection, and removes plants that have died or experienced reduced productivity. Planting healthy specimens, rather than damaged ones, can help compensate for crop losses.

Several models of PDT have been developed to illustrate how diseases spread and to identify contributing factors. Sisterson and Stenger [5] performed a sensitivity analysis on two spatial plant models and evaluated the effect of eliminating disease by reducing host-pathogen interactions. Nakasuji et al. [6] considered the PDT model as a system of ordinary differential equations (ODEs) by dividing the total population and vectors into three compartments each (healthy, latent infected, and infectious). Anggriani et al. [7] investigated the effect of preventive and curative fungicides on PDT. Their simulation results revealed the benefit of fungicides in reducing infected plants. Anggriani et al. [8] considered a mathematical model of PDT incorporating both curative and preventive interventions; they observed that the application of these treatments resulted in a deceleration of disease spread. In subsequent work, Anggriani et al. [9] developed a two-stage infection model, wherein both the latent and infectious plant compartments contribute to disease transmission within the population. This mechanism can accelerate the pace of PDT, as latent plants act as an additional source of infection alongside infectious plants [10]. In [11] the authors presented a FOM to describe plant epidemic dynamics, incorporating two control measures aimed at mitigating infection prevalence.

Fractional calculus was proposed in 1695 by Leibniz and has since developed into one of the very active topics of mathematics (see, e.g., [12–14]). Various definitions of fractional derivatives exist such as Grünwald–Letnikov, Riemann–Liouville, Caputo, Caputo–Fabrizio, and Atangana-Baleanu, which are widely used in applications of FDEs. Other definitions can be found in [15, 16] which do not generally match. In biological systems, the fractional order captures hereditary properties and memory effect that is gained from the non-locality of the fractional operator [17, 18], which offers a bridge between mathematical formalism and biological processes. Consequently, many researchers have attempted to describe real-world processes using different operators of fractional derivatives [19–24].

Fractional optimal control problems are another branch of mathematics that seeks to find optimal control trajectories and state variables that maximize or minimize a performance index (objective function). This index is typically represented by a fractional integral involving state variables and control trajectories, subject to constraint paths defined by a system of FDEs that describe the model's dynamics. To effectively solve FOCPs, certain NOCs should be satisfied. These conditions are established by a form of PMP, originally developed by the Russian mathematician Pontryagin [25]. In [26], authors used pathogen interaction factor with a pest invasion in a maize plant in the formulation of FOM and the influence of three controls on the transmission of this disease. In [27],

authors used quarantine, prevention, and insecticide chemical control efforts to eliminate the transmission dynamics of the maize streak virus. The authors in [28] proposed an advanced model of pine wilt disease and suggested three control efforts to minimize the infected pine trees and prevent disease transmission. There are many applications of FOCPs in various fields, as detailed in references (see, e.g., [29–31]) and related citations.

The main objective of the present study is to clarify the behavior of solutions to the plant disease model by implementing effective strategies for curative and preventive controls, and to bridge some gaps in the literature. Despite recent advancements in modeling plant disease dynamics using fractional calculus, critical gaps remain in the literature. First, prior fractional-order plant disease models, including those incorporating two-stage transmission [32], have overlooked the fundamental principle of dimensional consistency, where α introduces a time dimension that must be balanced across all parameters. Second, while the concept of two-stage transmission-where both latent and infectious plants contribute to disease spread-has been explored in integer-order contexts [9], its rigorous formulation and optimal control within a fractionally consistent framework have not been addressed. Third, no existing study has systematically investigated the combined effect of preventive and curative time-dependent controls within such a model, nor examined how the distinguishing transmission parameter ϵ influences optimal intervention strategies under varying memory effects. To bridge these gaps, this work introduces a novel fractional-order plant disease model that integrates three key contributions: (i) a dimensionally consistent formulation using the Caputo derivative, where all parameters are scaled by α to ensure physical and biological plausibility; (ii) a mathematical analysis, including existence, uniqueness, positivity, boundedness, and both local and global stability of equilibria, with R_c derived and analyzed for sensitivity; and (iii) FOCP that incorporates preventive and curative measures, solved numerically using FBSM based on a fractional Euler scheme. We examine the impact of the parameter $\epsilon \in (0, 1)$-which distinguishes the infectiousness of latent versus symptomatic plants-and α on disease dynamics and control efficacy.

The structure of this paper is as follows: The necessary concepts and definitions of fractional calculus are provided in Section 2. Section 3 describes the proposed FOM and discusses its qualitative analysis. Existence of solutions and their positivity and boundedness are mentioned in Subsection 3.1. Moreover, the stability and sensitivity analysis of the FOM are discussed in Subsections 3.2 and 3.3, respectively. The FOCP of the PDT is formulated based on a kind of PMP in Section 4. A numerical simulation of the obtained results for FOCP using FBSM is displayed in Section 5. Finally, the paper concludes in Section 6.

2. Preliminaries

Here, notations and definitions of fractional calculus are presented [33, 34]. Let $\mathbb{R}_+$ be a nonnegative real number set, then the Riemann-Liouville fractional integral (R-LFI) and Riemann-Liouville fractional derivative (RLFD) can be given as:

Definition 2.1. Let $g : \mathbb{R}_+ \longrightarrow \mathbb{R}$ be piecewise continuous on $\mathbb{R}_+$, then the R-LFI of order $\alpha > 0$ with t is described as

$$\text{(Left)} \quad {}_aI_t^{\alpha} g(t) = \frac{1}{\Gamma(\alpha)} \int_a^t (t-\tau)^{\alpha-1} g(\tau) d\tau,$$

$$\text{(Right)} \quad {}_tI_b^{\alpha} g(t) = \frac{1}{\Gamma(\alpha)} \int_t^b (\tau - t)^{\alpha-1} g(\tau) d\tau.$$

Definition 2.2. The RLFD is given as follows:

$$\text{(Left)} \quad {}_aD_t^{\alpha} g(t) = \frac{d^n}{dt^n} \left({}_aI_t^{n-\alpha} g(t)\right) = \frac{1}{\Gamma(n-\alpha)} \left(\frac{d}{dt}\right)^n \int_a^t (t - \tau)^{n-\alpha-1} g(\tau) d\tau,$$

$$\text{(Right)} \quad {}_tD_b^{\alpha} g(t) = (-\frac{d}{dt})^n \left({}_tI_b^{n-\alpha} g(t)\right) = \frac{1}{\Gamma(n-\alpha)} \left(-\frac{d}{dt}\right)^n \int_t^b (\tau - t)^{n-\alpha-1} g(\tau) d\tau,$$

where $\alpha \in (n-1, n)$; $n \in \mathbb{N}$.

Definition 2.3. The Caputo fractional derivative (CFD) for the function $g : \mathbb{R}_+ \longrightarrow \mathbb{R}$ is expressed as

$$\text{(Left)} \quad {}_a^C D_t^{\alpha} g(t) = \frac{1}{\Gamma(n-\alpha)} \int_a^t (t - \tau)^{n-\alpha-1} g^{(n)}(\tau) d\tau,$$

$$\text{(Right)} \quad {}_t^C D_b^{\alpha} g(t) = \frac{(-1)^n}{\Gamma(n-\alpha)} \int_t^b (\tau - t)^{n-\alpha-1} g^{(n)}(\tau) d\tau; \quad \alpha \in (n-1, n); n \in \mathbb{N}.$$

Theorem 2.1. *The RLFD and CFD are related by the following formulas:*

$$\begin{aligned} {}_aD_t^{\alpha} g(t) &= {}_a^C D_t^{\alpha} g(t) + \sum_{j=0}^{n-1} \frac{g^{(j)}(a)}{\Gamma(j-\alpha+1)} (t-a)^{(j-\alpha)}, \\ {}_tD_b^{\alpha} g(t) &= {}_t^C D_b^{\alpha} g(t) + \sum_{j=0}^{n-1} \frac{g^{(j)}(b)}{\Gamma(j-\alpha+1)} (b-t)^{(j-\alpha)}; \ t > 0, \alpha \in (n-1, n); n \in \mathbb{N}. \end{aligned}$$

The relation between the left and right of CFD is given by the following lemma.

Lemma 2.1. *For $t \in [a, b]$ and $\alpha \in (0, 1]$, the left and right CFD of fractional order α satisfies*

$${}_t^C D_b^{\alpha} g(t) = {}_a^C D_t^{\alpha} g(b - t).$$

A detailed proof of Lemma 2.1 can be found in [31, 35].

Definition 2.4. If $\mathfrak{L}\{g(t), s\} = G(s)$, then the Laplace transform (LT) for CFD of fractional order α is given as

$$\mathfrak{L}\{{}^C D^{\alpha} g(t), s\} = s^{\alpha} G(s) - \sum_{i=0}^{n-1} s^{\alpha-i-1} g^{(i)}(0), \quad (n-1 < \alpha \leq n); \ n \in \mathbb{N}.$$

Definition 2.5. ([36]) Mittag-Leffler function $\mathcal{M}_{l,m}(x)$; $x \in \mathbb{R}$, $l > 0$, $m > 0$, is defined by

$$\mathcal{M}_{l,m}(x) = \sum_{n=0}^{\infty} \frac{x^n}{\Gamma(ln + m)},$$

and the LT of $t^{m-1} \mathcal{M}_{l,m}(\pm \lambda t^l)$ is as follows:

$$\mathfrak{L}[t^{m-1} \mathcal{M}_{l,m}(\pm \lambda t^l)] = \frac{s^{l-m}}{s^l \mp \lambda}. \tag{2.1}$$

Also,

$$\mathcal{M}_{l,m}(x) = \frac{1}{\Gamma(m)} + x \, \mathcal{M}_{l,l+m}(x). \tag{2.2}$$

Definition 2.6. ([37]) The constant point x_i^*; $i = 1, 2, ..., n$, is an equilibrium point of the following nonlinear system of Caputo FDE:

$$\begin{aligned} {}_0^C D_t^\alpha x_i(t) &= f_i(x_1, x_2, ..., x_n, t), \quad 0 < \alpha < 1, \\ x_i(0) &= c_i, \end{aligned} \tag{2.3}$$

if, and only if, $f_i(t, x_i^*) = 0$.

Lemma 2.2. *([38]) The positive EPs of the system (2.3) are locally asymptotically stable (LAS) if all eigenvalues λ_i of its Jacobian matrix (JM) satisfy the following condition*

$$|arg(\lambda_i)| > \frac{\alpha\pi}{2}, \quad i =, 1, 2, ..., n. \tag{2.4}$$

Lemma 2.3. *The following formula is satisfied for the differentiable function $y(t) \in \mathbb{R}_+$*

$${}^C D_t^\alpha \left(y - y^* \ln \frac{y(t)}{y^*} - y^* \right) \leq \left(1 - \frac{y^*}{y(t)} \right) {}^C D_t^\alpha y(t), \quad y^* \in \mathbb{R}_+, \text{ for all } t \geq 0 \text{ and } \alpha \in (0, 1).$$

3. Formulation of the FOM and its qualitative analysis

The formulation of the FOM is presented, followed by a description of the transition dynamics among its compartments $\mathcal{S}(t)$, $\mathcal{P}(t)$, $\mathcal{L}(t)$, $\mathcal{I}(t)$, and $\mathcal{R}(t)$. The total plant population is given $\mathcal{N}(t) = \mathcal{S}(t) + \mathcal{P}(t) + \mathcal{L}(t) + \mathcal{I}(t) + \mathcal{R}(t)$. This formulation establishes the foundation for a comprehensive qualitative analysis. Subsequently, the EPs are evaluated, R_c is derived, and the theorems governing the local and global stability of these EPs are established.

Generally, the dynamics of PDT among these five compartments are interpreted based on standard epidemiological assumptions (see, e.g., [9, 32, 39]) to ensure the reliability of (3.1), as shown in Figure 1.

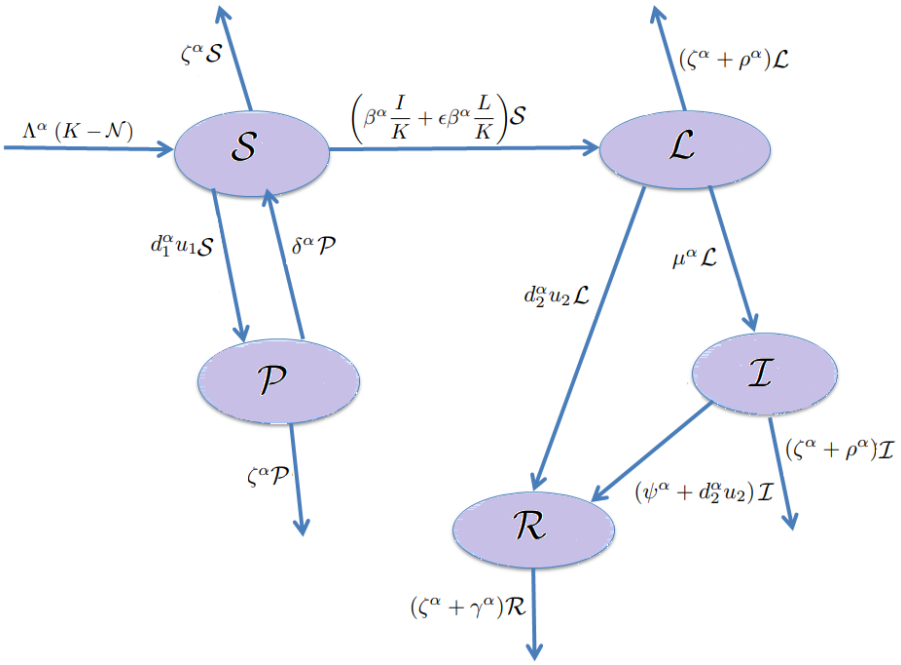

Figure 1. Flow chart diagram of the FOM (3.1).

The description of all parameters and remaining variables for the FOM are mentioned in Tables 1 and 2.

Table 1. Meanings of state variables with their initial values.

Variable	Definition	Initial value [9, 32, 39]
$\mathcal{S}(t)$	Susceptible plants at a time t	$\mathcal{S}(0) = \mathcal{S}_0 = 100$
$\mathcal{P}(t)$	Protected plants at a time t	$\mathcal{P}(0) = \mathcal{P}_0 = 30$
$\mathcal{L}(t)$	Latent plants at a time t	$\mathcal{L}(0) = \mathcal{L}_0 = 30$
$\mathcal{I}(t)$	Infected plants at a time t	$\mathcal{I}(0) = \mathcal{I}_0 = 60$
$\mathcal{R}(t)$	Removed plants at a time t	$\mathcal{R}(0) = \mathcal{R}_0 = 60$

Table 2. Interpretation of dynamic transformation and values of the parameters in FOM.

Parameter	Description	Value	Reference
Λ^α	Replanting rate of $\mathcal{S}(t)$	$(0.013)^\alpha$	[40]
ρ^α	Roguing rate of $\mathcal{I}(t)$	$(0.087)^\alpha$	[40, 41]
β^α	Rate of PDT from $\mathcal{I}(t)$ to $\mathcal{S}(t)$	$(0.3)^\alpha$	[7]
ψ^α	Conversion rate from $\mathcal{I}(t)$ to $\mathcal{R}(t)$	$(0.02)^\alpha$	[9, 39]
ζ^α	Natural mortality rate of $\mathcal{S}(t)$	$(0.0008)^\alpha$	[40]
μ^α	Conversion rate from $\mathcal{L}(t)$ to $\mathcal{I}(t)$	$(0.17)^\alpha$	[8]
γ^α	Effect cumulative death rates for $\mathcal{R}(t)$	$(0.01)^\alpha$	[9, 39]
d_1^α	Measure efficacy of preventive treatment u_1	$(0.5)^\alpha$	Assumed
d_2^α	Measure efficacy of curative treatment u_2	$(0.5)^\alpha$	Assumed
δ^α	Damage rate caused of u_1	$(0.048)^\alpha$	[9, 39]
K	Total capacity of plants	1000	[40]
ϵ	Distinguishing factor in two-stage transmission; $\epsilon \in (0, 1)$	Varying	Assumed

Following all the above assumptions, the framework of two-stage disease transmission dynamics in plants is considered as:

$$\begin{cases} {}_0^C D_t^\alpha \mathcal{S}(t) = \Lambda^\alpha\,(K - \mathcal{N}) - \left(\beta^\alpha \dfrac{\mathcal{I}(t)}{K} + \epsilon\beta^\alpha \dfrac{\mathcal{L}(t)}{K}\right)\mathcal{S}(t) - (\zeta^\alpha + d_1^\alpha u_1)\mathcal{S}(t) + \delta^\alpha \mathcal{P}(t), \\ {}_0^C D_t^\alpha \mathcal{P}(t) = d_1^\alpha u_1 \mathcal{S}(t) - (\delta^\alpha + \zeta^\alpha)\mathcal{P}(t), \\ {}_0^C D_t^\alpha \mathcal{L}(t) = \left(\beta^\alpha \dfrac{\mathcal{I}(t)}{K} + \epsilon\,\beta^\alpha \dfrac{\mathcal{L}(t)}{K}\right)\mathcal{S}(t) - (\zeta^\alpha + \rho^\alpha + \mu^\alpha + d_2^\alpha u_2)\mathcal{L}(t), \\ {}_0^C D_t^\alpha \mathcal{I}(t) = \mu^\alpha \mathcal{L}(t) - (\zeta^\alpha + \rho^\alpha + \psi^\alpha + d_2^\alpha u_2)\mathcal{I}(t), \\ {}_0^C D_t^\alpha \mathcal{R}(t) = (\psi^\alpha + d_2^\alpha u_2)\mathcal{I}(t) - (\zeta^\alpha + \gamma^\alpha)\mathcal{R}(t) + d_2^\alpha u_2 \mathcal{L}(t), \end{cases} \tag{3.1}$$

subject to the initial conditions (ICs) mentioned in Table 1. Now, the model is formulated as a system of FDEs, which effectively means the dynamics have "memory" as opposed to being driven solely by the current state as in an ODE formulation. This formalism (usually with $\alpha \to 1$) is used primarily

because the classical order PDT epidemic (that is, $\alpha = 1$) does not provide any information regarding the memory impact and the learning process of the disease that influences its spread [42].

3.1. Solution existence, positivity, and boundedness

Based on the idea of converting the FOM (3.1) with the nonnegative ICs into fractional integral equations, the fixed point theory is used to prove that a unique solution of the FOM (3.1) exists. As Lemma 5.2 in [36], the equivalent fractional integral forms of (3.1) are

$$\begin{cases} \mathcal{S}(t) = \mathcal{S}_0 + \dfrac{1}{\Gamma(\alpha)}\displaystyle\int_0^t (t-\tau)^{\alpha-1} f_1(\tau, \mathcal{S}(\tau))d\tau, \\ \mathcal{P}(t) = \mathcal{P}_0 + \dfrac{1}{\Gamma(\alpha)}\displaystyle\int_0^t (t-\tau)^{\alpha-1} f_2(\tau, \mathcal{P}(\tau))d\tau, \\ \mathcal{L}(t) = \mathcal{L}_0 + \dfrac{1}{\Gamma(\alpha)}\displaystyle\int_0^t (t-\tau)^{\alpha-1} f_3(\tau, \mathcal{L}(\tau))d\tau, \\ \mathcal{I}(t) = \mathcal{I}_0 + \dfrac{1}{\Gamma(\alpha)}\displaystyle\int_0^t (t-\tau)^{\alpha-1} f_4(\tau, \mathcal{I}(\tau))d\tau, \\ \mathcal{R}(t) = \mathcal{R}_0 + \dfrac{1}{\Gamma(\alpha)}\displaystyle\int_0^t (t-\tau)^{\alpha-1} f_5(\tau, \mathcal{R}(\tau))d\tau, \end{cases} \tag{3.2}$$

where

$$\begin{cases} f_1(t, \mathcal{S}(t)) = \Lambda^\alpha\ (K - \mathcal{N}) - \Big(\beta^\alpha \dfrac{\mathcal{I}(t)}{K} + \epsilon\beta^\alpha \dfrac{\mathcal{L}(t)}{K}\Big)\mathcal{S}(t) - (\zeta^\alpha + d_1^\alpha u_1)\mathcal{S}(t) + \delta^\alpha \mathcal{P}(t), \\ f_2(t, \mathcal{P}(t)) = d_1^\alpha u_1 \mathcal{S}(t) - (\zeta^\alpha + \delta^\alpha)\mathcal{P}(t), \\ f_3(t, \mathcal{L}(t)) = \Big(\beta^\alpha \dfrac{\mathcal{I}(t)}{K} + \epsilon\,\beta^\alpha \dfrac{\mathcal{L}(t)}{K}\Big)\mathcal{S}(t) - (\zeta^\alpha + \rho^\alpha + \mu^\alpha + d_2^\alpha u_2)\mathcal{L}(t), \\ f_4(t, \mathcal{I}(t)) = \mu^\alpha \mathcal{L}(t) - (\zeta^\alpha + \rho^\alpha + \psi^\alpha + d_2^\alpha u_2)\mathcal{I}(t), \\ f_5(t, \mathcal{R}(t)) = (\psi^\alpha + d_2^\alpha u_2)\mathcal{I}(t) - (\zeta^\alpha + \gamma^\alpha)R(t) + d_2^\alpha u_2 \mathcal{L}(t), \end{cases} \tag{3.3}$$

and $f_1,\ f_2,\ f_3,\ f_4$, and f_5 are continuous nonlinear functions. In the following theorem, the kernel f_1 is defined, where all parameters are positive and $0 < \alpha < 1$.

Theorem 3.1. *If* $\Big(\dfrac{\beta^\alpha}{K}(b_4 + \epsilon b_3) + \zeta^\alpha + d_1^\alpha u_1\Big) < 1$, *and assuming that the state variables of FOM (3.1) are bounded, then* f_1 *satisfies the Lipschitz condition and contraction.*

Proof. Let $(\mathcal{S}, \mathcal{P}, \mathcal{L}, \mathcal{I}, \mathcal{R}) \in E$ be the set of solution, where $E = [C(I, \mathbb{R}_+)]^5;\ I = [0, T]$ is a Banach space together with the norm induced metric $\|.\|_E$ and $\mathcal{S}, \mathcal{S}_1$ satisfy Eq (3.1) and its initial value, giving

$$\begin{aligned} \|f_1(t, \mathcal{S}) - f_1(t, \mathcal{S}_1)\| &= \left\| -\Big(\beta^\alpha \frac{\mathcal{I}(t)}{K} + \epsilon\beta^\alpha \frac{\mathcal{L}(t)}{K}\Big)(\mathcal{S}(t) - \mathcal{S}_1(t)) - (\zeta^\alpha + d_1^\alpha u_1)(\mathcal{S}(t) - \mathcal{S}_1(t))\right\| \\ &\le \left\|\beta^\alpha \frac{\mathcal{I}(t)}{K} + \epsilon\beta^\alpha \frac{\mathcal{L}(t)}{K}\right\| \|\mathcal{S}(t) - \mathcal{S}_1(t)\| + (\zeta^\alpha + d_1^\alpha u_1)\|\mathcal{S}(t) - \mathcal{S}_1(t)\| \\ &\le \Big(\frac{\beta^\alpha}{K}\|\mathcal{I}(t)\| + \epsilon\frac{\beta^\alpha}{K}\|\mathcal{L}(t)\| + \zeta^\alpha + d_1^\alpha u_1\Big)\|\mathcal{S}(t) - \mathcal{S}_1(t)\| \\ &\le \Big(\frac{\beta^\alpha}{K} b_4 + \epsilon\frac{\beta^\alpha}{K} b_3 + \zeta^\alpha + d_1^\alpha u_1\Big)\|\mathcal{S}(t) - \mathcal{S}_1(t)\|, \end{aligned}$$

where $\|\mathcal{I}(t)\| \leq b_4,\ \|\mathcal{L}(t)\| \leq b_3$ are bounded functions; and let $h_1 = (\frac{\beta^\alpha}{K}(b_4 + \epsilon b_3) + \zeta^\alpha + d_1^\alpha u_1)$, then

$$\|f_1(t, \mathcal{S}) - f_1(t, \mathcal{S}_1)\| \leq h_1 \|\mathcal{S}(t) - \mathcal{S}_1(t)\|. \tag{3.4}$$

Thus, f_1 satisfies Lipschitz, and if $0 \leq h_1 < 1$, then f_1 is a contraction.

By the same way, $f_i;\ i = 2, 3, 4, 5$, can be written as

$$\begin{cases} \|f_2(t, \mathcal{P}) - f_2(t, \mathcal{P}_1)\| \leq h_2 \|\mathcal{P}(t) - \mathcal{P}_1(t)\|, \\ \|f_3(t, \mathcal{L}) - f_3(t, \mathcal{L}_1)\| \leq h_3 \|\mathcal{L}(t) - \mathcal{L}_1(t)\|, \\ \|f_4(t, \mathcal{I}) - f_4(t, \mathcal{I}_1)\| \leq h_4 \|\mathcal{I}(t) - \mathcal{I}_1(t)\|, \\ \|f_5(t, \mathcal{R}) - f_5(t, \mathcal{R}_1)\| \leq h_5 \|\mathcal{R}(t) - \mathcal{R}_1(t)\|, \end{cases} \tag{3.5}$$

where $h_2 = \delta^\alpha + \zeta^\alpha,\ h_3 = (\frac{\epsilon\beta^\alpha}{K} b_1 + \zeta^\alpha + \rho^\alpha + \mu^\alpha + d_2^\alpha u_2),\ h_4 = \zeta^\alpha + \rho^\alpha + \psi^\alpha + d_2^\alpha u_2,\ h_5 = \zeta^\alpha + \gamma^\alpha$ and $\|\mathcal{S}(t)\| \leq b_1$ is bounded function. Now, the kernels $f_i;\ i = 2, 3, 4, 5$ are a contraction, whenever $0 \leq h_i < 1$ for all $i = 2, 3, 4, 5$.

Theorem 3.2. *There exists a unique solution to the FOM (3.1), whenever* $(1 - \frac{h_i t}{\Gamma(\alpha)}) > 0$*; i* $= 1, 2, 3, 4, 5$.

Proof. According to the system (3.2), the following recurrence forms are obtained:

$$\begin{aligned} Q_{1n}(t) &= \mathcal{S}_n(t) - \mathcal{S}_{n-1}(t) = \frac{1}{\Gamma(\alpha)} \int_0^t (t-\tau)^{\alpha-1} (f_1(\tau, \mathcal{S}_{n-1}) - f_1(\tau, \mathcal{S}_{n-2})) d\tau, \\ Q_{2n}(t) &= \mathcal{P}_n(t) - \mathcal{P}_{n-1}(t) = \frac{1}{\Gamma(\alpha)} \int_0^t (t-\tau)^{\alpha-1} (f_2(\tau, \mathcal{P}_{n-1}) - f_2(\tau, \mathcal{P}_{n-2})) d\tau, \\ Q_{3n}(t) &= \mathcal{L}_n(t) - \mathcal{L}_{n-1}(t) = \frac{1}{\Gamma(\alpha)} \int_0^t (t-\tau)^{\alpha-1} (f_3(\tau, \mathcal{L}_{n-1}) - f_3(\tau, \mathcal{L}_{n-2})) d\tau, \\ Q_{4n}(t) &= \mathcal{I}_n(t) - \mathcal{I}_{n-1}(t) = \frac{1}{\Gamma(\alpha)} \int_0^t (t-\tau)^{\alpha-1} (f_4(\tau, \mathcal{L}_{n-1}) - f_4(\tau, \mathcal{L}_{n-2})) d\tau, \\ Q_{5n}(t) &= \mathcal{R}_n(t) - \mathcal{R}_{n-1}(t) = \frac{1}{\Gamma(\alpha)} \int_0^t (t-\tau)^{\alpha-1} (f_5(\tau, \mathcal{R}_{n-1}) - f_5(\tau, \mathcal{R}_{n-2})) d\tau, \end{aligned} \tag{3.6}$$

with the positive ICs. For the first equation,

$$\begin{aligned} \|Q_{1n}(t)\| &= \|\mathcal{S}_n(t) - \mathcal{S}_{n-1}(t)\| \\ &= \frac{1}{\Gamma(\alpha)} \| \int_0^t (f_1(\tau, \mathcal{S}_{n-1}) - f_1(\tau, \mathcal{S}_{n-2}))\ (t-\tau)^{\alpha-1} d\tau \| \\ &\leq \frac{1}{\Gamma(\alpha)} \int_0^t \|(f_1(\tau, \mathcal{S}_{n-1}) - f_1(\tau, \mathcal{S}_{n-2}))\|\ (t-\tau)^{\alpha-1} d\tau. \end{aligned}$$

From Lipschitz condition (3.4), thus

$$\|Q_{1n}(t)\| \leq \frac{h_1}{\Gamma(\alpha)} \int_0^t \|Q_{1(n-1)}(\tau)\| d\tau. \tag{3.7}$$

In the same way, it gives

$$\begin{cases} \|Q_{2n}(t)\| \leq \dfrac{h_2}{\Gamma(\alpha)}\displaystyle\int_0^t \|Q_{2(n-1)}(\tau)\|d\tau, \\ \|Q_{3n}(t)\| \leq \dfrac{h_3}{\Gamma(\alpha)}\displaystyle\int_0^t \|Q_{3(n-1)}(\tau)\|d\tau, \\ \|Q_{4n}(t)\| \leq \dfrac{h_4}{\Gamma(\alpha)}\displaystyle\int_0^t \|Q_{4(n-1)}(\tau)\|d\tau, \\ \|Q_{5n}(t)\| \leq \dfrac{h_5}{\Gamma(\alpha)}\displaystyle\int_0^t \|Q_{5(n-1)}(\tau)\|d\tau. \end{cases} \tag{3.8}$$

Terms of the projected solution can be given as

$$\mathcal{S}_n(t) = \sum_{i=0}^{n} Q_{1i}(t),\ \ \mathcal{P}_n(t) = \sum_{i=0}^{n} Q_{2i}(t),\ \ \mathcal{L}_n(t) = \sum_{i=0}^{n} Q_{3i}(t),\ \ \mathcal{I}_n(t) = \sum_{i=0}^{n} Q_{4i}(t),\ \mathcal{R}_n(t) = \sum_{i=0}^{n} Q_{5i}(t).$$

From the iterative technique and Eqs (3.7) and (3.8), it leads to

$$\begin{aligned} \|Q_{1n}(t)\| &\leq \left(\frac{h_1 t}{\Gamma(\alpha)}\right)^n \|\mathcal{S}_n(0)\|, \\ \|Q_{2n}(t)\| &\leq \left(\frac{h_2 t}{\Gamma(\alpha)}\right)^n \|\mathcal{P}_n(0)\|, \\ \|Q_{3n}(t)\| &\leq \left(\frac{h_3 t}{\Gamma(\alpha)}\right)^n \|\mathcal{L}_n(0)\|, \\ \|Q_{4n}(t)\| &\leq \left(\frac{h_4 t}{\Gamma(\alpha)}\right)^n \|\mathcal{I}_n(0)\|, \\ \|Q_{5n}(t)\| &\leq \left(\frac{h_5 t}{\Gamma(\alpha)}\right)^n \|\mathcal{R}_n(0)\|. \end{aligned}$$

Now, it is established that the system has a continuous solution. To clarify that the above functions construct a solution of (3.2), assume that

$$\begin{cases} \mathcal{S}(t) - \mathcal{S}(0) = \mathcal{S}_n(t) - \mathcal{B}_{1n}(t), \\ \mathcal{P}(t) - \mathcal{P}(0) = \mathcal{P}_n(t) - \mathcal{B}_{2n}(t), \\ \mathcal{L}(t) - \mathcal{L}(0) = \mathcal{L}_n(t) - \mathcal{B}_{3n}(t), \\ \mathcal{I}(t) - \mathcal{I}(0) = \mathcal{I}_n(t) - \mathcal{B}_{4n}(t), \\ \mathcal{R}(t) - \mathcal{R}(0) = \mathcal{R}_n(t) - \mathcal{B}_{5n}(t). \end{cases}$$

Thus,

$$\begin{aligned} \|\mathcal{B}_{1n}(t)\| &= \|\frac{1}{\Gamma(\alpha)}\int_0^t (f_1(\tau,\mathcal{S}) - f_1(\tau,\mathcal{S}_{n-1}))(t-\tau)^{\alpha-1}d\tau\| \\ &\leq \frac{1}{\Gamma(\alpha)}\int_0^t \|(f_1(\tau,\mathcal{S}) - f_1(\tau,\mathcal{S}_{n-1}))(t-\tau)^{\alpha-1}\|d\tau \\ &\leq \frac{h_1}{\Gamma(\alpha)}\|\mathcal{S} - \mathcal{S}_{n-1}\|t. \end{aligned}$$

Repeating this technique gives (at $t = t_1$)

$$\|\mathcal{B}_{1n}(t)\| \leq \left(\frac{t_1}{\Gamma(\alpha)}\right)^{n+1} h_1^{n+1} k. \tag{3.9}$$

The limit of Eq (3.9) at $n \to 0$ tends to $\|\mathcal{B}_{1n}(t)\| \to 0$. This yields $\|\mathcal{B}_{in}(t)\| \to 0$; $i = 2, 3, 4, 5$. This means completing the proof of existence. To show the solution is unique, let $(\mathcal{S}_1(t), \mathcal{P}_1(t), \mathcal{L}_1(t), \mathcal{I}_1(t), \mathcal{R}_1(t))$ be another solution set of the FOM (3.1), which yields

$$\mathcal{S}(t) - \mathcal{S}_1(t) = \frac{1}{\Gamma(\alpha)} \int_0^t (f_1(\tau, \mathcal{S}) - f_1(\tau, \mathcal{S}_1))(t-\tau)^{\alpha-1} d\tau.$$

The norm of the above equation with Lipschitz condition (3.4) gives

$$\|\mathcal{S}(t) - \mathcal{S}_1(t)\| \leq \frac{h_1 t}{\Gamma(\alpha)} \|\mathcal{S}(t) - \mathcal{S}_1(t)\|.$$

Thus,

$$\|\mathcal{S}(t) - \mathcal{S}_1(t)\| \left(1 - \frac{h_1 t}{\Gamma(\alpha)}\right) \leq 0 \implies \|\mathcal{S}(t) - \mathcal{S}_1(t)\| = 0 \implies \mathcal{S}(t) = \mathcal{S}_1(t).$$

By the same way, get $\mathcal{P}(t) = \mathcal{P}_1(t), \mathcal{L}(t) = \mathcal{L}_1(t), \mathcal{I}(t) = \mathcal{I}_1(t)$, and $\mathcal{R}(t) = \mathcal{R}_1(t)$.

Theorem 3.3. *The set of solution $(\mathcal{S}(t), \mathcal{P}(t), \mathcal{L}(t), \mathcal{I}(t), \mathcal{R}(t))$ is nonnegative for all $t \geq 0$, if the set of ICs $(\mathcal{S}(0), \mathcal{P}(0), \mathcal{L}(0), \mathcal{I}(0), \mathcal{R}(0))$ are positive values.*

Proof. From the susceptible equation:

$$\begin{aligned} {}_0^C D_t^\alpha \mathcal{S}(t) &= (K - \mathcal{N})\, \Lambda^\alpha - \left(\frac{\mathcal{I}(t)}{K} + \epsilon \frac{\mathcal{L}(t)}{K}\right) \beta^\alpha \mathcal{S}(t) - (\zeta^\alpha + d_1^\alpha u_1) \mathcal{S}(t) + \delta^\alpha \mathcal{P}(t), \\ &\geq -(\zeta^\alpha + d_1^\alpha u_1) S(t). \end{aligned} \tag{3.10}$$

Applying LT on both sides of Eq (3.10) and from Eq (2.1), we get

$$\mathcal{S}(t) \geq \mathcal{S}_0\, \mathcal{M}_{\alpha,1}(-(\zeta^\alpha + d_1^\alpha u_1) t^\alpha) > 0, \quad \forall\ t > 0.$$

The inequalities below confirmed that the remaining state variables are positive.

$$\begin{aligned} \mathcal{P}(t) &\geq \mathcal{P}_0\, \mathcal{M}_{\alpha,1}(-(\delta^\alpha + \zeta^\alpha) t^\alpha) \geq 0, \\ \mathcal{L}(t) &\geq \mathcal{L}_0\, \mathcal{M}_{\alpha,1}(-(\zeta^\alpha + \rho^\alpha + \mu^\alpha + d_2^\alpha u_2) t^\alpha) \geq 0, \quad \forall\ t > 0. \\ \mathcal{I}(t) &\geq \mathcal{I}_0\, \mathcal{M}_{\alpha,1}(-(\zeta^\alpha + \rho^\alpha + \psi^\alpha + d_2^\alpha u_2) t^\alpha) \geq 0, \\ \mathcal{R}(t) &\geq \mathcal{R}_0\, \mathcal{M}_{\alpha,1}(-(\zeta^\alpha + \gamma^\alpha) t^\alpha) \geq 0. \end{aligned}$$

Theorem 3.4. *The solution of* (3.1) *is bounded and remains in* $\Theta = \{(\mathcal{S}, \mathcal{P}, \mathcal{L}, \mathcal{I}, \mathcal{R}) \in \mathbb{R}_+^5; 0 < \mathcal{N} \leq \frac{\Lambda^\alpha K}{\mu^\alpha + \Lambda^\alpha}\}$.

Proof. Let the set $\Theta = \{(\mathcal{S}, \mathcal{P}, \mathcal{L}, \mathcal{I}, \mathcal{R}) \in \mathbb{R}_+^5\}$ be any solution of the FOM (3.1) with the initial population $\mathcal{N}(0) = \mathcal{S}_0 + \mathcal{P}_0 + \mathcal{L}_0 + \mathcal{I}_0 + \mathcal{R}_0 > 0$. The FDE of $\mathcal{N}(t)$ can be obtained by addition of Eq (3.1), as follows:

$$\begin{aligned} {}^{C}_{0}D^{\alpha}_{t}\mathcal{N}(t) &= \Lambda^{\alpha}K - (\zeta^{\alpha}+\Lambda^{\alpha})\mathcal{N}(t) - \rho^{\alpha}(\mathcal{I}(t)+\mathcal{L}(t)) - \gamma^{\alpha}\mathcal{R}(t) \\ &\leq \Lambda^{\alpha}K - (\zeta^{\alpha}+\Lambda^{\alpha})\mathcal{N}(t). \end{aligned} \tag{3.11}$$

Using LT on both sides of Eq (3.11),

$$\begin{aligned} s^{\alpha}\bar{\mathcal{N}}(s) - s^{\alpha-1}\mathcal{N}(0) &\leq \frac{\Lambda^{\alpha}K}{s} - (\zeta^{\alpha}+\Lambda^{\alpha})\bar{\mathcal{N}}(s) \\ \bar{\mathcal{N}}(s) &\leq \frac{\Lambda^{\alpha}K}{s(s^{\alpha}+\zeta^{\alpha}+\Lambda^{\alpha})} + \frac{s^{\alpha-1}}{s^{\alpha}+\zeta^{\alpha}+\Lambda^{\alpha}}\mathcal{N}(0). \end{aligned} \tag{3.12}$$

Applying inverse LT on Eq (3.12) and from Eqs (2.2) and (2.1), leads to

$$\mathcal{N}(t) \leq \Lambda^{\alpha}Kt^{\alpha}\ E_{\alpha,\alpha+1}(-(\zeta^{\alpha}+\Lambda^{\alpha})t^{\alpha}) + E_{\alpha,1}(-(\zeta^{\alpha}+\Lambda^{\alpha})t^{\alpha})\ \mathcal{N}(0).$$

From the properties of the Mittag-Leffler function [33], we have $\lim_{t\to\infty}\mathcal{N}(t) \leq \frac{\Lambda^{\alpha}K}{\zeta^{\alpha}+\Lambda^{\alpha}}$. Thus, $0 < \mathcal{N} \leq \frac{\Lambda^{\alpha}K}{\mu^{\alpha}+\Lambda^{\alpha}}$, which means that Θ is the largest set in which $\mathcal{S}(t), \mathcal{P}(t), \mathcal{L}(t), \mathcal{I}(t)$, and $\mathcal{R}(t)$ are bounded.

3.2. Local and global stability

To analyze the stability of FOM (3.1), all possible EPs are identified and R_c is computed as follows:

Disease-free equilibrium (DFE) point $\Xi^{*} = (\mathcal{S}^{*}_{eq}, \mathcal{P}^{*}_{eq}, \mathcal{L}^{*}_{eq}, \mathcal{I}^{*}_{eq}, \mathcal{R}^{*}_{eq})$: in this point, no infection was detected (i.e., $\mathcal{I} = 0$), then substituting in Eq (3.1) leads to

$$\Xi^{*} = \left(\frac{\Lambda^{\alpha}K(\zeta^{\alpha}+\delta^{\alpha})}{(\zeta^{\alpha}+\Lambda^{\alpha})(\zeta^{\alpha}+\delta^{\alpha}+d^{\alpha}_{1}u_{1})}, \frac{\Lambda^{\alpha}Kd^{\alpha}_{1}u_{1}}{(\zeta^{\alpha}+\Lambda^{\alpha})(\zeta^{\alpha}+\delta^{\alpha}+d^{\alpha}_{1}u_{1})}, 0, 0, 0\right). \tag{3.13}$$

Using the the next-generation matrix approach (see, e.g., [43, 44]), R_c is given by

$$R_c = \sqrt{\frac{\Lambda^{\alpha}\beta^{\alpha}\mu^{\alpha}(\zeta^{\alpha}+\delta^{\alpha})}{(\zeta^{\alpha}+\rho^{\alpha}+\psi^{\alpha}+d^{\alpha}_{2}u_{2})[(\zeta^{\alpha}+\Lambda^{\alpha})(\zeta^{\alpha}+\rho^{\alpha}+\mu^{\alpha}+d^{\alpha}_{2}u_{2})(\zeta^{\alpha}+\delta^{\alpha}+d^{\alpha}_{1}u_{1}) - \epsilon\beta^{\alpha}\Lambda^{\alpha}(\zeta^{\alpha}+\delta^{\alpha})]}}. \tag{3.14}$$

Endemic equilibrium point (EEP) $\Xi^{**} = (\mathcal{S}^{**}_{eq}, \mathcal{P}^{**}_{eq}, \mathcal{L}^{**}_{eq}, \mathcal{I}^{**}_{eq}, \mathcal{R}^{**}_{eq})$: in the endemic steady state (i.e., $\mathcal{I} \neq 0$), its corresponding equilibrium point can be written as follows:

$$\begin{cases} \mathcal{S}^{**}_{eq} = \dfrac{K(\zeta^{\alpha}+a)(\zeta^{\alpha}+b)}{\beta^{\alpha}\mu^{\alpha}+\epsilon\beta^{\alpha}(\zeta^{\alpha}+b)}, \\ \mathcal{P}^{**}_{eq} = \dfrac{Kd^{\alpha}_{1}u_{1}(\zeta^{\alpha}+a)(\zeta^{\alpha}+b)}{(\beta^{\alpha}\mu^{\alpha}+\epsilon\beta^{\alpha}(\zeta^{\alpha}+b))(\zeta^{\alpha}+\delta^{\alpha})}, \\ \mathcal{L}^{**}_{eq} = \dfrac{\Lambda^{\alpha}(\beta^{\alpha}\mu^{\alpha}+\epsilon\beta^{\alpha}(\zeta^{\alpha}+b))(K-N)(\zeta^{\alpha}+\delta^{\alpha}) - K\zeta^{\alpha}(\zeta^{\alpha}+a)(\zeta^{\alpha}+b)(\zeta^{\alpha}+d)}{(\beta^{\alpha}\mu^{\alpha}+\epsilon\beta^{\alpha}(\zeta^{\alpha}+b))(\zeta^{\alpha}+\delta^{\alpha})(\zeta^{\alpha}+a)}, \\ \mathcal{I}^{**}_{eq} = \dfrac{\Lambda^{\alpha}\mu^{\alpha}(\beta^{\alpha}\mu^{\alpha}+\epsilon\beta^{\alpha}(\zeta^{\alpha}+b))(K-N)(\zeta^{\alpha}+\delta^{\alpha}) - \mu^{\alpha}K\zeta^{\alpha}(\zeta^{\alpha}+a)(\zeta^{\alpha}+b)(\zeta^{\alpha}+d)}{(\beta^{\alpha}\mu^{\alpha}+\epsilon\beta^{\alpha}(\zeta^{\alpha}+b))(\zeta^{\alpha}+\delta^{\alpha})(\zeta^{\alpha}+a)(\mu^{\alpha}+b)}, \\ \mathcal{R}^{*}_{eq} = \dfrac{\mu^{\alpha}(\psi^{\alpha}+d^{\alpha}_{2}u_{2})[\Lambda^{\alpha}(\beta^{\alpha}\mu^{\alpha}+\epsilon\beta^{\alpha}(\zeta^{\alpha}+b))(K-N)(\zeta^{\alpha}+\delta^{\alpha}) - K\zeta^{\alpha}(\zeta^{\alpha}+a)(\zeta^{\alpha}+b)(\zeta^{\alpha}+d)]}{(\beta^{\alpha}\mu^{\alpha}+\epsilon\beta^{\alpha}(\zeta^{\alpha}+b))(\zeta^{\alpha}+\delta^{\alpha})(\zeta^{\alpha}+a)(\mu^{\alpha}+b)(\zeta^{\alpha}+\gamma^{\alpha})}, \end{cases} \tag{3.15}$$

where, $a = \rho^\alpha + \mu^\alpha + d_2^\alpha u_2,\ b = \rho^\alpha + \psi^\alpha + d_2^\alpha u_2$, and $d = \delta^\alpha + d_1^\alpha u_1$.

Local stability: The investigation of LAS for Ξ^* (3.13) and Ξ^{**} (3.15) is stated and proved by the following theorems:

Theorem 3.5. *The DFE Ξ^* of (3.1) is LAS whenever $R_c < 1$, otherwise, it is unstable.*

Proof. The JM at Ξ^* is given by

$$\mathbb{J}_{\Xi^*_{eq}} = \begin{bmatrix} -(\zeta^\alpha + d_1^\alpha u_1) & \delta^\alpha & \frac{-\epsilon\Lambda^\alpha\beta^\alpha(\zeta^\alpha+\delta^\alpha)}{(\zeta^\alpha+\Lambda^\alpha)(\zeta^\alpha+d)} & \frac{-\Lambda^\alpha\beta^\alpha(\zeta^\alpha+\delta^\alpha)}{(\zeta^\alpha+\Lambda^\alpha)(\zeta^\alpha+d)} & 0 \\ d_1^\alpha u_1 & -(\zeta^\alpha+\delta^\alpha) & 0 & 0 & 0 \\ 0 & 0 & -(\zeta^\alpha+a)+\frac{\epsilon\Lambda^\alpha\beta^\alpha(\zeta^\alpha+\delta^\alpha)}{(\zeta^\alpha+\Lambda^\alpha)(\zeta^\alpha+d)} & \frac{\Lambda^\alpha\beta^\alpha(\zeta^\alpha+\delta^\alpha)}{(\zeta^\alpha+\Lambda^\alpha)(\zeta^\alpha+d)} & 0 \\ 0 & 0 & \mu^\alpha & -(\zeta^\alpha+b) & 0 \\ 0 & 0 & d_2^\alpha u_2 & \psi^\alpha + d_2^\alpha u_2 & -(\zeta^\alpha+\gamma^\alpha) \end{bmatrix}.$$

By calculating the eigenvalues of $\mathbb{J}_{\Xi^*_{eq}}$, thus $\chi_1 = -(\zeta^\alpha + \gamma^\alpha) < 0$, satisfied the condition $|\arg(\chi_i)| = \pi > \frac{\alpha\pi}{2}$ (Lemma 2.2). The following quadratic equations give the remaining eigenvalues:

$$\chi^2 + (2\zeta^\alpha + \delta^\alpha + d_1^\alpha u_1)\chi + (\zeta^\alpha+\delta^\alpha)(\zeta^\alpha + d_1^\alpha u_1) - \delta^\alpha d_1^\alpha u_1 = 0, \tag{3.16}$$

and

$$\lambda^2 + \Big((\zeta^\alpha+b)(\zeta^\alpha+a) - \frac{\epsilon\Lambda^\alpha\beta^\alpha(\zeta^\alpha+\delta^\alpha)}{(\zeta^\alpha+\Lambda^\alpha)(\zeta^\alpha+d)}\Big)\lambda + \frac{(\zeta^\alpha+b)[(\zeta^\alpha+\Lambda^\alpha)(\zeta^\alpha+a)(\zeta^\alpha+d) - \epsilon\beta^\alpha\Lambda^\alpha(\zeta^\alpha+\delta^\alpha)]}{(\zeta^\alpha+\Lambda^\alpha)(\zeta^\alpha+d)}(1-R_c^2) = 0. \tag{3.17}$$

From Eqs (3.16) and (3.17), observe that

- For LAS, it must be $R_c < 1$; this means that all coefficients of the quadratic polynomials (3.16) and (3.17) have the same signal, then the eigenvalues have negative real part [45].

Theorem 3.6. *The FOM (3.1) at the EEP Ξ^{**}_{eq} is LAS under some conditions obtained from Routh-Hurwitz criteria, for a particular set of parameter values (as given in Table 2).*

Proof. The JM of (3.1) evaluated at the EEP Ξ^{**}_{eq} is given by:

$$\mathbb{J}_{\Xi^{**}_{eq}} = \begin{bmatrix} -\mathcal{K}_1 & \delta^\alpha & -\frac{\epsilon\beta^\alpha\mathcal{S}^{**}_{eq}}{K} & -\frac{\beta^\alpha\mathcal{S}^{**}_{eq}}{K} & 0 \\ d_1^\alpha u_1 & -(\zeta^\alpha+\delta^\alpha) & 0 & 0 & 0 \\ \mathcal{K}_2 & 0 & -(\zeta^\alpha+a)+\frac{\epsilon\beta^\alpha\mathcal{S}^{**}_{eq}}{K} & \frac{\beta^\alpha\mathcal{S}^{**}_{eq}}{K} & 0 \\ 0 & 0 & \mu^\alpha & -(\zeta^\alpha+b) & 0 \\ 0 & 0 & d_2^\alpha u_2 & \psi^\alpha + d_2^\alpha u_2 & -(\zeta^\alpha+\gamma^\alpha) \end{bmatrix},$$

where $\mathcal{K}_1 = \zeta^\alpha + d_1^\alpha u_1 + \frac{\beta^\alpha\mathcal{I}^{**}_{eq}}{K} + \frac{\epsilon\beta^\alpha\mathcal{L}^{**}_{eq}}{K}$, $\mathcal{K}_2 = \frac{\beta^\alpha\mathcal{I}^{**}_{eq}}{K} + \frac{\epsilon\beta^\alpha\mathcal{L}^{**}_{eq}}{K}$. One eigenvalue of $\mathbb{J}_{\Xi^{**}_{eq}}$ is $\Lambda_1 = -(\zeta^\alpha+\gamma^\alpha) < 0$, which satisfies the condition $|\arg(\Lambda_1)| = \pi > \frac{\alpha\pi}{2}$ (Lemma 2.2). The remaining four eigenvalues are the roots of the following characteristic polynomial:

$$\Lambda^4 + \mathcal{A}_1\Lambda^3 + \mathcal{A}_2\Lambda^2 + \mathcal{A}_3\Lambda + \mathcal{A}_4 = 0, \tag{3.18}$$

where the coefficients $\mathcal{A}_i$ $(i = 1, 2, 3, 4)$ are:

$$\begin{aligned}
\mathcal{A}_1 &= \mathcal{K}_1 + 3\zeta^\alpha + \delta^\alpha + a + b - \frac{\epsilon\beta^\alpha \mathcal{S}^{**}_{eq}}{K},\\
\mathcal{A}_2 &= \mathcal{K}_1\Big(3\zeta^\alpha + \delta^\alpha + a + b - \frac{\epsilon\beta^\alpha \mathcal{S}^{**}_{eq}}{K}\Big) + (\zeta^\alpha + b)\Big(2\zeta^\alpha + \delta^\alpha + a - \frac{\epsilon\beta^\alpha \mathcal{S}^{**}_{eq}}{K}\Big)\\
&\quad - \frac{\beta^\alpha \mathcal{S}^{**}_{eq}}{K}\Big(\mu^\alpha + \epsilon(\zeta^\alpha + \delta^\alpha - \mathcal{K}_2)\Big) + (\zeta^\alpha + \delta^\alpha)(\zeta^\alpha + a) - \delta^\alpha d_1^\alpha u_1,\\
\mathcal{A}_3 &= \mathcal{K}_1\Big[(\zeta^\alpha + b)\Big(2\zeta^\alpha + \delta^\alpha + a - \frac{\epsilon\beta^\alpha \mathcal{S}^{**}_{eq}}{K}\Big) - \frac{\beta^\alpha \mathcal{S}^{**}_{eq}}{K}(\mu^\alpha + \epsilon(\zeta^\alpha + \delta^\alpha)) + (\zeta^\alpha + \delta^\alpha)(\zeta^\alpha + a)\Big]\\
&\quad + (\zeta^\alpha + b)\Big[(\zeta^\alpha + \delta^\alpha)(\zeta^\alpha + a) - \delta^\alpha d_1^\alpha u_1 + \frac{\epsilon\beta^\alpha \mathcal{S}^{**}_{eq}}{K}(\mathcal{K}_2 - (\zeta^\alpha + \delta^\alpha))\Big]\\
&\quad + \frac{\beta^\alpha \mathcal{S}^{**}_{eq}}{K}\Big[\mu^\alpha(\mathcal{K}_2 - (\zeta^\alpha + \delta^\alpha)) + \epsilon((\zeta^\alpha + \delta^\alpha)\mathcal{K}_2 + \delta^\alpha d_1^\alpha u_1)\Big] - \delta^\alpha d_1^\alpha u_1(\zeta^\alpha + a),\\
\mathcal{A}_4 &= \mathcal{K}_1\Big[(\zeta^\alpha + \delta^\alpha)(\zeta^\alpha + a)(\zeta^\alpha + b) - \frac{\beta^\alpha \mathcal{S}^{**}_{eq}}{K}(\zeta^\alpha + \delta^\alpha)(\mu^\alpha + \epsilon(\zeta^\alpha + b))\Big]\\
&\quad + \frac{\beta^\alpha \mathcal{S}^{**}_{eq}}{K}(\mathcal{K}_2(\zeta^\alpha + \delta^\alpha) + \delta^\alpha d_1^\alpha u_1)(\mu^\alpha + \epsilon(\zeta^\alpha + b)) - \delta^\alpha d_1^\alpha u_1(\zeta^\alpha + a)(\zeta^\alpha + b).
\end{aligned} \tag{3.19}$$

For the parameter values specified in Table 2, we compute the coefficients $\mathcal{A}_1, \mathcal{A}_2, \mathcal{A}_3, \mathcal{A}_4$ given in Eq (3.19) (see Appendix A). All coefficients are found to be positive, and the inequality $\mathcal{A}_1\mathcal{A}_2\mathcal{A}_3 > \mathcal{A}_3^2 + \mathcal{A}_1^2\mathcal{A}_4$ whenever $R_c > 1$ is satisfied. Consequently, according to the Routh-Hurwitz stability criteria [45], the characteristic polynomial (3.18) has roots with negative real parts, implying that the EEP Ξ^{**}_{eq} is LAS when $R_c > 1$ for this parameter configuration. It should be noted that this verification is performed for the specific parameter set used in our numerical simulations.

Global stability: The global stability of Ξ^{*}_{eq} (3.13) and Ξ^{**} (3.15) for the FOM (3.1) discusses as follows:

Theorem 3.7. *The DFE Ξ^{*}_{eq} of (3.1) is global asymptotically stable (GAS).*

Proof. Consider the following positive Lyapunov function on Θ

$$\mathbb{L}_1(\mathcal{S}, \mathcal{P}, \mathcal{L}, \mathcal{I}, \mathcal{R}) = \Big(\mathcal{S} - \mathcal{S}^*_{eq} - \mathcal{S}^*_{eq} \ln \frac{\mathcal{S}}{\mathcal{S}^*_{eq}}\Big) + \Big(\mathcal{P} - \mathcal{P}^*_{eq} - \mathcal{P}^*_{eq} \ln \frac{\mathcal{P}}{\mathcal{P}^*_{eq}}\Big).$$

and from Eq (3.1) and Lemma (2.3), we get

$$\begin{aligned}
{}^{C}_{0}D^\alpha_t \mathbb{L}_1(\mathcal{S}, \mathcal{P}, \mathcal{L}, \mathcal{I}, \mathcal{R}) &\leq \Big(\frac{\mathcal{S} - \mathcal{S}^*_{eq}}{\mathcal{S}}\Big) {}^{C}_{0}D^\alpha_t \mathcal{S} + \Big(\frac{\mathcal{P} - \mathcal{P}^*_{eq}}{\mathcal{P}}\Big) {}^{C}_{0}D^\alpha_t \mathcal{P}\\
&= \Big(\frac{\mathcal{S} - \mathcal{S}^*_{eq}}{\mathcal{S}}\Big)\Big[\Lambda^\alpha\,(K - \mathcal{N}) - \Big(\beta^\alpha \frac{\mathcal{I}}{K} + \epsilon\beta^\alpha \frac{\mathcal{L}}{K}\Big)\mathcal{S} - (\zeta^\alpha + d_1^\alpha u_1)\mathcal{S} + \delta^\alpha \mathcal{P}\Big]\\
&\quad + \Big(\frac{\mathcal{P} - \mathcal{P}^*_{eq}}{\mathcal{P}}\Big)\Big[d_1^\alpha u_1 \mathcal{S} - (\delta^\alpha + \zeta^\alpha)\mathcal{P}\Big].
\end{aligned}$$

At Ξ^{*}_{eq}, thus,

$$
\begin{aligned}
{}_0^C D_t^\alpha \mathbb{L}_1(\mathcal{S},\mathcal{P},\mathcal{L},\mathcal{I},\mathcal{R}) &\leq (\mathcal{S}-\mathcal{S}^*_{eq})\Big(\tfrac{\Lambda^\alpha\ (K-\mathcal{N})}{\mathcal{S}}+\tfrac{\delta^\alpha\mathcal{P}}{\mathcal{S}}-(\zeta^\alpha+d_1^\alpha u_1)\Big)+(\mathcal{P}-\mathcal{P}^*_{eq})\Big(\tfrac{d_1^\alpha u_1\mathcal{S}}{\mathcal{P}}-(\delta^\alpha+\zeta^\alpha)\Big)\\
&= (\mathcal{S}-\mathcal{S}^*_{eq})\Big(\tfrac{\Lambda^\alpha\ (K-\mathcal{N})}{S}+\tfrac{\delta^\alpha\mathcal{P}}{\mathcal{S}}-\tfrac{\Lambda^\alpha\ (K-\mathcal{N})}{\mathcal{S}^*_{eq}}-\tfrac{\delta^\alpha\mathcal{P}}{\mathcal{S}^*_{eq}}\Big)+(\mathcal{P}-\mathcal{P}^*_{eq})\Big(\tfrac{d_1^\alpha u_1\mathcal{S}}{\mathcal{P}}-\tfrac{d_1^\alpha u_1\mathcal{S}}{\mathcal{P}^*_{eq}}\Big)\\
&= (\mathcal{S}-\mathcal{S}^*_{eq})\Big(-\tfrac{\Lambda^\alpha\ (K-\mathcal{N})}{\mathcal{S}\,\mathcal{S}^*_{eq}}(\mathcal{S}-\mathcal{S}^*_{eq})-\tfrac{\delta^\alpha\mathcal{P}}{\mathcal{S}\,\mathcal{S}^*_{eq}}(\mathcal{S}-\mathcal{S}^*_{eq})\Big)+(\mathcal{P}-\mathcal{P}^*_{eq})\Big(-\tfrac{d_1^\alpha u_1\mathcal{S}}{\mathcal{P}\,\mathcal{P}^*_{eq}}(\mathcal{P}-\mathcal{P}^*_{eq})\Big).
\end{aligned}
$$

Thus,

$$
{}_0^C D_t^\alpha \mathbb{L}_1(\mathcal{S},\mathcal{P},\mathcal{L},\mathcal{I},\mathcal{R}) \leq -\frac{\Lambda^\alpha\ (K-\mathcal{N})}{\mathcal{S}\,\mathcal{S}^*_{eq}}(\mathcal{S}-\mathcal{S}^*_{eq})^2-\frac{\delta^\alpha\mathcal{P}}{\mathcal{S}\,\mathcal{S}^*_{eq}}(\mathcal{S}-\mathcal{S}^*_{eq})^2-\frac{d_1^\alpha u_1\mathcal{S}}{\mathcal{P}\,\mathcal{P}^*_{eq}}(\mathcal{P}-\mathcal{P}^*_{eq})^2.
$$

For each solution $(\mathcal{S},\mathcal{P},\mathcal{L},\mathcal{I},\mathcal{R})\in\Theta$, conclude that ${}_0^C D_t^\alpha \mathbb{L}_1<0$. Furthermore, ${}_0^C D_t^\alpha \mathbb{L}_1=0$ implies that $\mathcal{S}=\mathcal{S}^*_{eq}$, $\mathcal{P}=\mathcal{P}^*_{eq}$, $\mathcal{L}=\mathcal{L}^*_{eq}$, $\mathcal{I}=\mathcal{I}^*_{eq}$, and $\mathcal{R}=\mathcal{R}^*_{eq}$. Hence, Ξ^*_{eq} is the only invariant subset of Θ such that ${}_0^C D_t^\alpha \mathbb{L}_1=0$ and from fractional LaSalle's invariance principle [46, 47], the EEP Ξ^*_{eq} is GAS on Θ.

Theorem 3.8. *The unique positive EEP Ξ^{**}_{eq} of (3.1) is GAS.*

Proof. The Lyapunov function can be considered as:

$$
\begin{aligned}
\mathbb{L}_2(\mathcal{S},\mathcal{P},\mathcal{L},\mathcal{I},\mathcal{R}) &= \Big(\mathcal{S}-\mathcal{S}^{**}_{eq}-\mathcal{S}^{**}_{eq}\ln\frac{\mathcal{S}}{\mathcal{S}^{**}_{eq}}\Big)+\Big(\mathcal{P}-\mathcal{P}^{**}_{eq}-\mathcal{P}^{**}_{eq}\ln\frac{\mathcal{P}}{\mathcal{P}^{**}_{eq}}\Big)+\Big(\mathcal{L}-\mathcal{L}^{**}_{eq}-\mathcal{L}^{**}_{eq}\ln\frac{\mathcal{L}}{\mathcal{L}^{**}_{eq}}\Big)\\
&+ \Big(\mathcal{I}-\mathcal{I}^{**}_{eq}-\mathcal{I}^{**}_{eq}\ln\frac{\mathcal{I}}{\mathcal{I}^{**}_{eq}}\Big)+\Big(\mathcal{R}-\mathcal{R}^{*}_{eq}-\mathcal{R}^{**}_{eq}\ln\frac{\mathcal{R}}{\mathcal{R}^{**}_{eq}}\Big).
\end{aligned}
$$

From Lemma (2.3) and Eq (3.1), one obtains

$$
\begin{aligned}
{}_0^C D_t^\alpha \mathbb{L}_2(\mathcal{S},\mathcal{P},\mathcal{L},\mathcal{I},\mathcal{R}) &\leq \Big(\tfrac{\mathcal{S}-\mathcal{S}^{**}_{eq}}{\mathcal{S}}\Big)\Big[\Lambda^\alpha\ (K-\mathcal{N})-\Big(\beta^\alpha\frac{\mathcal{I}}{K}+\epsilon\beta^\alpha\frac{\mathcal{L}}{K}\Big)\mathcal{S}-(\zeta^\alpha+d_1^\alpha u_1)\mathcal{S}+\delta^\alpha\mathcal{P}\Big]+\Big(\tfrac{\mathcal{P}-\mathcal{P}^{**}_{eq}}{\mathcal{P}}\Big)\\
&\times \Big[d_1^\alpha u_1\mathcal{S}-(\delta^\alpha+\zeta^\alpha)\mathcal{P}\Big]+\Big(\tfrac{L-\mathcal{L}^{**}_{eq}}{\mathcal{L}}\Big)\Big[\Big(\beta^\alpha\frac{\mathcal{I}}{K}+\epsilon\beta^\alpha\frac{\mathcal{L}}{K}\Big)\mathcal{S}-(\zeta^\alpha+\rho^\alpha+\mu^\alpha+d_2^\alpha u_2)\mathcal{L}\Big]\\
&+ \Big(\frac{\mathcal{I}-\mathcal{I}^{**}_{eq}}{\mathcal{I}}\Big)\Big[\mu^\alpha\mathcal{L}-(\zeta^\alpha+\rho^\alpha+\psi^\alpha+d_2^\alpha u_2)\mathcal{I}\Big]+\Big(\frac{\mathcal{R}-\mathcal{R}^{**}_{eq}}{\mathcal{R}}\Big)\\
&\times \Big[(\psi^\alpha+d_2^\alpha u_2)\mathcal{I}-(\zeta^\alpha+\gamma^\alpha)\mathcal{R}+d_2^\alpha u_2\mathcal{L}\Big]. \qquad (3.20)
\end{aligned}
$$

Eq (3.20) can be written as

$$
\begin{aligned}
{}_0^C D_t^\alpha \mathbb{L}_2(\mathcal{S},\mathcal{P},\mathcal{L},\mathcal{I},\mathcal{R}) &\leq (\mathcal{S}-\mathcal{S}^{**}_{eq})\Big(\tfrac{\Lambda^\alpha\ (K-\mathcal{N})}{\mathcal{S}}+\tfrac{\delta^\alpha\mathcal{P}}{\mathcal{S}}-(\zeta^\alpha+d_1^\alpha u_1)\Big)+(\mathcal{P}-\mathcal{P}^{**}_{eq})\Big(\tfrac{d_1^\alpha u_1\mathcal{S}}{\mathcal{P}}-(\delta^\alpha+\zeta^\alpha)\Big)\\
&+ (\mathcal{L}-\mathcal{L}^{**}_{eq})\Big(\frac{\beta^\alpha\mathcal{S}\mathcal{I}}{\mathcal{L}K}-(\zeta^\alpha+\rho^\alpha+\mu^\alpha+d_2^\alpha u_2)\Big)+(\mathcal{I}-\mathcal{I}^{**}_{eq})\Big(\tfrac{\mu^\alpha\mathcal{L}}{\mathcal{I}}-(\zeta^\alpha+\rho^\alpha+\psi^\alpha+d_2^\alpha u_2)\Big)\\
&+ (\mathcal{R}-\mathcal{R}^{**}_{eq})\Big(\frac{\psi^\alpha\mathcal{I}}{\mathcal{R}}+\frac{d_2^\alpha u_2\mathcal{I}}{\mathcal{R}}+\frac{d_2^\alpha u_2\mathcal{L}}{\mathcal{R}}-(\zeta^\alpha+\gamma^\alpha)\Big). \qquad (3.21)
\end{aligned}
$$

Rearranging Eq (3.21) and performing simple calculations yields:

$$
\begin{aligned}
{}_0^C D_t^\alpha \mathbb{L}_2(\mathcal{S},\mathcal{P},\mathcal{L},\mathcal{I},\mathcal{R}) \quad \leq \quad & -\tfrac{\Lambda^\alpha\,(K-N)}{\mathcal{S}\mathcal{S}^{**}_{eq}}(\mathcal{S}-\mathcal{S}^{**}_{eq})^2 - \tfrac{\delta^\alpha \mathcal{P}}{\mathcal{S}\mathcal{S}^{**}_{eq}}(\mathcal{S}-\mathcal{S}^{**}_{eq})^2 - \tfrac{d_1^\alpha u_1 \mathcal{S}}{\mathcal{P}\mathcal{P}^{**}_{eq}}(\mathcal{P}-\mathcal{P}^{**}_{eq})^2 - \frac{\beta^\alpha \mathcal{S}\mathcal{I}}{\mathcal{L}\mathcal{L}^{**}_{eq}K}(\mathcal{L}-\mathcal{L}^{**}_{eq})^2 \\
& - \frac{\mu^\alpha \mathcal{L}}{\mathcal{I}\mathcal{I}^{**}_{eq}}(\mathcal{I}-\mathcal{I}^{**}_{eq})^2 - \left(\frac{(\psi^\alpha + d_2^\alpha u_2)\mathcal{I}}{\mathcal{R}\mathcal{R}^{**}_{eq}} + \frac{d_2^\alpha u_2 \mathcal{L}}{\mathcal{R}\mathcal{R}^{**}_{eq}}\right)(\mathcal{R}-\mathcal{R}^{**}_{eq})^2.
\end{aligned}
$$

Thus, ${}_0^C D_t^\alpha \mathbb{L}_2 < 0$, for all $(\mathcal{S},\mathcal{I},\mathcal{P},\mathcal{L},\mathcal{I},\mathcal{R}) \in \Theta$. Furthermore, ${}_0^C D_t^\alpha \mathbb{L}_2 = 0$ means that $\mathcal{S} = \mathcal{S}^{**}_{eq}$, $\mathcal{P} = \mathcal{P}^{**}_{eq}$, $\mathcal{I} = \mathcal{I}^{**}_{eq}$, $\mathcal{L} = \mathcal{L}^{**}_{eq}$, $\mathcal{I} = \mathcal{I}^{**}_{eq}$, and $\mathcal{R} = \mathcal{R}^{**}_{eq}$. As a result, utilizing fractional LaSalle's invariance principle, then Ξ^{**}_{eq} is GAS on Θ.

3.3. Sensitivity indicator

To determine which of the parameters listed in Eq (3.14) impact R_0 (in the absence of control) and consequently influence disease transmission, a sensitivity analysis is conducted. This is achieved using the following sensitivity index [48, 49]:

$$
\mathbb{E}^{R_0}_{\varpi} = \frac{\partial R_0}{\partial \varpi} \times \frac{\varpi}{R_0},
$$

where ϖ are the parameters in R_0. For example, sensitivity index for parameters Λ and ρ is given by

$$
\mathbb{E}^{R_0}_{\Lambda} = \frac{\alpha\zeta^\alpha\,(\zeta^\alpha + \mu^\alpha + \rho^\alpha)}{2\left(\Lambda^\alpha\,(-\epsilon\beta^\alpha + \mu^\alpha + \rho^\alpha) + \zeta^{2\alpha} + \zeta^\alpha\,(\Lambda^\alpha + \mu^\alpha + \rho^\alpha)\right)} > 0,
$$

$$
\mathbb{E}^{R_0}_{\rho} = -\frac{\alpha\rho^\alpha\left(\Lambda^\alpha\,(-\epsilon\beta^\alpha + \mu^\alpha + 2\rho^\alpha + \psi^\alpha) + 2\zeta^{2\alpha} + \zeta^\alpha\,(2\Lambda^\alpha + \mu^\alpha + 2\rho^\alpha + \psi^\alpha)\right)}{2\left(\zeta^\alpha + \rho^\alpha + \psi^\alpha\right)\left(\Lambda^\alpha\,(-\epsilon\beta^\alpha + \mu^\alpha + \rho^\alpha) + \zeta^{2\alpha} + \zeta^\alpha\,(\Lambda^\alpha + \mu^\alpha + \rho^\alpha)\right)} < 0,
$$

it is straightforward to calculate the rest of the remaining parameters similarly. Note that, the positive (negative) value for the sensitivity index has an expulsive (reverse) effect on R_0, which means that a positive (negative) index reveals that any change in these parameter values leads to an increase (decrease) of R_0. Consequently, the propagation of the disease in plants increases (decreases). The values of $\mathbb{E}^{R_0}_{\varpi}$ for the model parameters are displayed in Figure 2(a). From the presented results, the most directly sensitive parameter is β, followed by ϵ, then Λ, and the most inversely sensitive parameter is ρ, followed by μ, then ψ and ζ. This indicates that, for example, if both β, ϵ and Λ were to increase or (decrease) by 10%, then the value of R_0 would increase or (decrease) by 11.0648%, 6.06479%, and 0.641437%, respectively. In contrast, if both ρ, μ, ψ, and ζ were to increase or (decrease) by 10%, then the value of R_0 would decrease or (increase) by 7.7693%, 2.29641%, 0.927644%, and 0.712879%, respectively.

Figure 2(c),(d) shows the influence of Λ and ρ on R_0, any decrease in Λ and increase in ρ, followed by a decrease in the value of R_0. Moreover, the effect of changing Λ and ρ on $\mathcal{I}(t)$ is presented in Figure 2(b) with different values of α. It becomes clear that as the value of Λ and α decreases and the value of ρ increases, the infected plants are reduced. From the explanations provided, it is necessary to use control strategies and suggest optimal control elements that can effectively reduce the possibility of disease transmission and its spread in plants.

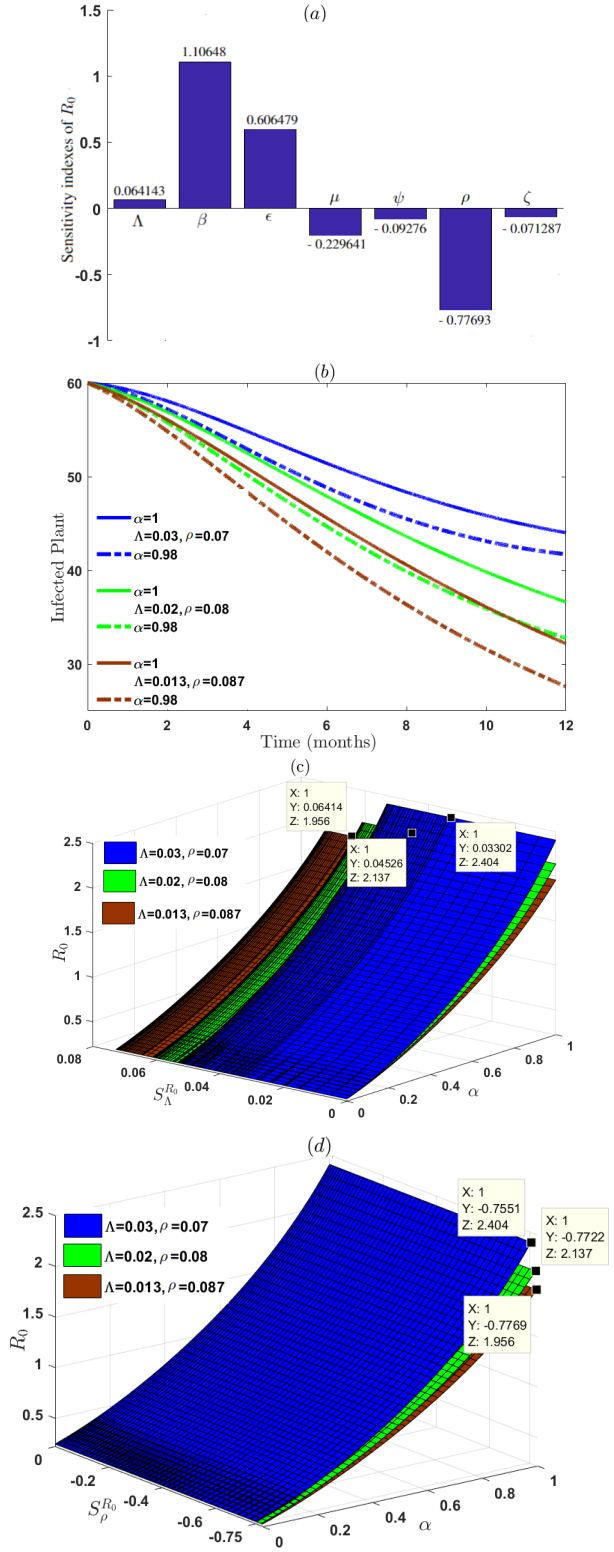

Figure 2. (a) Sensitivity analysis of R_0. (b)–(d) Influence of Λ, ρ, and α in sensitivity indicator.

4. Control problem formulation

$$\text{Minimize} \quad J(u_1, u_2) = {}_0I_T^{\alpha}\Psi(\mathcal{S}, \mathcal{P}, \mathcal{L}, \mathcal{I}, \mathcal{R}, u_1, u_2, t), \tag{4.1}$$

where

$$\Psi(\mathcal{S}, \mathcal{P}, \mathcal{L}, \mathcal{I}, \mathcal{R}, u_1, u_2, t) = A_1\mathcal{I}(t) + A_2\mathcal{L}(t) + \sum_{k=1}^{2} \frac{C_k}{2} u_k^2(t),$$

${}_0I_T^{\alpha}$ is the R-LFI of order $0 < \alpha \leq 1$, A_1 and A_2 are the weight factors for $\mathcal{I}(t)$ and $\mathcal{L}(t)$, respectively, and $C_k; k = 1, 2$ are weights for $u_k(t)$, which can be adjusted based on sensitivity results to prioritize control efforts on the most influential compartments ($\mathcal{I}(t)$ and $\mathcal{L}(t)$). Subject to the dynamic constraints

$${}_0^C D_t^{\alpha}\Xi(t) = Y(\mathcal{S}, \mathcal{P}, \mathcal{L}, \mathcal{I}, \mathcal{R}, u_1, u_2, t), \tag{4.2}$$

where

$$\Xi = \begin{pmatrix} \mathcal{S} \\ \mathcal{P} \\ \mathcal{I} \\ \mathcal{L} \\ \mathcal{R} \end{pmatrix} \qquad \text{and} \qquad Y = \begin{pmatrix} Y_1 \\ Y_2 \\ Y_3 \\ Y_4 \\ Y_5 \end{pmatrix};$$

$$\begin{aligned}
Y_1 &= \Lambda^{\alpha}(K - N) - \left(\beta^{\alpha}\frac{\mathcal{I}(t)}{K} + \epsilon\beta^{\alpha}\frac{\mathcal{L}(t)}{K}\right)\mathcal{S}(t) - (\zeta^{\alpha} + d_1^{\alpha}u_1)\mathcal{S}(t) + \delta^{\alpha}\mathcal{P}(t), \\
Y_2 &= d_1^{\alpha}u_1\mathcal{S}(t) - (\delta^{\alpha} + \zeta^{\alpha})\mathcal{P}(t), \\
Y_3 &= \left(\beta^{\alpha}\frac{\mathcal{I}(t)}{K} + \epsilon\beta^{\alpha}\frac{\mathcal{L}(t)}{K}\right)\mathcal{S}(t) - (\zeta^{\alpha} + \rho^{\alpha} + \mu^{\alpha} + d_2^{\alpha}u_2)\mathcal{L}(t), \\
Y_4 &= \mu^{\alpha}\mathcal{L}(t) - (\zeta^{\alpha} + \rho^{\alpha} + \psi^{\alpha} + d_2^{\alpha}u_2)\mathcal{I}(t), \\
Y_5 &= (\psi^{\alpha} + d_2^{\alpha}u_2)\mathcal{I}(t) - (\gamma^{\alpha} + \zeta^{\alpha})\mathcal{R}(t) + d_2^{\alpha}u_2\mathcal{L}(t),
\end{aligned}$$

subject to nonnegative ICs in Table 1. The set of admissible controls is specified by:

$$\mathcal{U} = \{u_i(t); i = 1, 2 \text{ and } u_1, u_2 \text{ are Lebesgue measurable with } 0 \leq u_i(t) \leq 1, t \in I\}.$$

Depending on the kind of PMP for FOCPs [25, 50], the Hamiltonian H can be formulated as:

$$H(\mathcal{S}, \mathcal{P}, \mathcal{L}, \mathcal{I}, \mathcal{R}, u_1, u_2, P, t) = \Psi(\mathcal{S}, \mathcal{P}, \mathcal{L}, \mathcal{I}, \mathcal{R}, u_1, u_2, t) + P(t)Y(\mathcal{S}, \mathcal{P}, \mathcal{L}, \mathcal{I}, \mathcal{R}, u_1, u_2, t), \tag{4.3}$$

where $P(t)$ is the adjoint vector defined by

$$P(t) = (p_1(t), p_2(t), p_3(t), p_4(t), p_5(t)). \tag{4.4}$$

The required NOCs of this FOCP are offered in the next theorem.

Theorem 4.1. *For given optimal controls (u_1^*, u_2^*) and optimal solutions $(\mathcal{S}^*, \mathcal{P}^*, \mathcal{L}^*, \mathcal{I}^*, \mathcal{R}^*)$ of the state dynamical system (4.2). Consequently, there exists $P(t)$ (4.4), which satisfies:*

$$\begin{aligned}
{}_0^C D_t^\alpha p_1(t^*) &= \Big(p_3(t^*) - p_1(t^*)\Big)\Big(\beta^\alpha \frac{\mathcal{I}(t^*)}{K} + \epsilon\beta^\alpha \frac{\mathcal{L}(t^*)}{K}\Big) + d_1^\alpha u_1(t^*)\Big(p_2(t^*) - p_1(t^*)\Big) - \zeta^\alpha p_1(t^*),\\
{}_0^C D_t^\alpha p_2(t^*) &= \delta^\alpha\Big(p_1(t^*) - p_2(t^*)\Big) - \zeta^\alpha p_2(t^*),\\
{}_0^C D_t^\alpha p_3(t^*) &= A_2 + \epsilon\beta^\alpha \frac{\mathcal{S}(t^*)}{K}\Big(p_3(t^*) - p_1(t^*)\Big) + \mu^\alpha\Big(p_4(t^*) - p_3(t^*)\Big) + d_2^\alpha u_2(t^*)\Big(p_5(t^*) - p_3(t^*)\Big)\\
&\quad -(\zeta^\alpha + \rho^\alpha)p_3(t^*),\\
{}_0^C D_t^\alpha p_4(t^*) &= A_1 + \beta^\alpha \frac{\mathcal{S}(t^*)}{K}\Big(p_3(t^*) - p_1(t^*)\Big) + (\psi^\alpha + d_2^\alpha u_2(t^*))\Big(p_5(t^*) - p_4(t^*)\Big) - (\zeta^\alpha + \rho^\alpha)p_4(t^*),\\
{}_0^C D_t^\alpha p_5(t^*) &= -(\zeta^\alpha + \gamma^\alpha)p_5(t^*),
\end{aligned} \tag{4.5}$$

where $t^* = T - t$, with the transversality conditions

$$P(T) = 0. \tag{4.6}$$

Furthermore, for $u_i^*; i = 1, 2$ minimizing proposed FOCP over $\mathcal{U}$, thus

$$H(\mathcal{S}^*, \mathcal{P}^*, \mathcal{L}^*, \mathcal{I}^*, \mathcal{R}^*, u_1^*, u_2^*, P, t) = \min_{0\le u_1, u_2 \le 1} H(\mathcal{S}^*, \mathcal{P}^*, \mathcal{L}^*, \mathcal{I}^*, \mathcal{R}^*, u_1, u_2, P, t),$$

such that

$$\begin{aligned}
u_1^*(t) &= \min\{\max\{0, \frac{(p_1(t) - p_2(t))d_1^\alpha \mathcal{S}^*(t)}{C_1}\}, 1\},\\
u_2^*(t) &= \min\{\max\{0, \frac{(p_3(t) - p_5(t))d_2^\alpha \mathcal{L}^*(t) + (p_4(t) - p_5(t))d_2^\alpha \mathcal{I}^*(t)}{C_2}\}, 1\}.
\end{aligned} \tag{4.7}$$

Proof. According to Eq (4.3), the Hamiltonian with optimal variables can be written as:

$$\begin{aligned}
H(\mathcal{S}^*, \mathcal{P}^*, \mathcal{L}^*, \mathcal{I}^*, \mathcal{R}^*, u_1^*, u_2^*, P, t) = A_1\mathcal{I}(t) + A_2\mathcal{L}(t) + \sum_{k=1}^{2} \frac{C_k}{2} u_k^2(t) + p_1(t)Y_1(\mathcal{S}^*, \mathcal{P}^*, \mathcal{L}^*, \mathcal{I}^*, \mathcal{R}^*, u_1^*, u_2^*, t)\\
+p_2(t)Y_2(\mathcal{S}^*, \mathcal{P}^*, \mathcal{L}^*, \mathcal{I}^*, \mathcal{R}^*, u_1^*, u_2^*, t) + p_3(t)Y_3(\mathcal{S}^*, \mathcal{P}^*, \mathcal{L}^*, \mathcal{I}^*, \mathcal{R}^*, u_1^*, u_2^*, t)\\
+p_4(t)Y_4(\mathcal{S}^*, \mathcal{P}^*, \mathcal{L}^*, \mathcal{I}^*, \mathcal{R}^*, u_1^*, u_2^*, t) + p_5(t)Y_5(\mathcal{S}^*, \mathcal{P}^*, \mathcal{L}^*, \mathcal{I}^*, \mathcal{R}^*, u_1^*, u_2^*, t).
\end{aligned}$$

Based on the kind of PMP [25], if $u_1^*, u_2^* \in \mathcal{U}$, then it is optimal for the FOCP (4.1) and (4.2) with ICs. This leads to

$$\begin{aligned}
{}_t D_{t_f}^\alpha p_1(t) &= \frac{\partial H(\mathcal{S}^*, \mathcal{P}^*, \mathcal{L}^*, \mathcal{I}^*, \mathcal{R}^*, u_1^*, u_2^*, P, t)}{\partial S^*}\\
&= (p_3(t) - p_1(t))\Big(\beta^\alpha \frac{\mathcal{I}^*(t)}{K} + \epsilon\beta^\alpha \frac{\mathcal{L}^*(t)}{K}\Big) + d_1^\alpha u_1^*(t)(p_2(t) - p_1(t)) - \zeta^\alpha p_1(t),
\end{aligned}$$

$$
\begin{aligned}
{}_tD^{\alpha}_{t_f} p_2(t) &= \frac{\partial H(\mathcal{S}^*, \mathcal{P}^*, \mathcal{L}^*, \mathcal{I}^*, \mathcal{R}^*, u_1^*, u_2^*, P, t)}{\partial P^*} = \delta^{\alpha}(p_1(t) - p_2(t)) - \zeta^{\alpha} p_2(t), \qquad (4.8)\\
{}_tD^{\alpha}_{t_f} p_3(t) &= \frac{\partial H(S^*, P^*, L^*, I^*, R^*, u_1^*, u_2^*, \mathcal{P}, t)}{\partial L^*}\\
&= A_2 + \epsilon\beta^{\alpha}\frac{\mathcal{S}^*(t)}{K}(p_3(t) - p_1(t)) + \mu^{\alpha}(p_4(t) - p_3(t)) + d_2^{\alpha}u_2^*(t)(p_5(t) - p_3(t)) - (\zeta^{\alpha} + \rho^{\alpha})p_3(t),\\
{}_tD^{\alpha}_{t_f} p_4(t) &= \frac{\partial H(\mathcal{S}^*, \mathcal{P}^*, \mathcal{L}^*, \mathcal{I}^*, \mathcal{R}^*, u_1^*, u_2^*, P, t)}{\partial I^*}\\
&= A_1 + \beta^{\alpha}\frac{\mathcal{S}^*(t)}{K}(p_3(t) - p_1(t)) + (\psi^{\alpha} + d_2^{\alpha}u_2^*(t))(p_5(t) - p_4(t)) - (\zeta^{\alpha} + \rho^{\alpha})p_4(t),\\
{}_tD^{\alpha}_{t_f} p_5(t) &= \frac{\partial H(\mathcal{S}^*, \mathcal{P}^*, \mathcal{L}^*, \mathcal{I}^*, \mathcal{R}^*, u_1^*, u_2^*, P, t)}{\partial R^*} = -(\zeta^{\alpha} + \gamma^{\alpha})p_5(t),
\end{aligned}
$$

with the transversality conditions

$$p_1(T) = 0, \qquad p_2(T) = 0, \qquad p_3(T) = 0, \qquad p_4(T) = 0, \qquad p_5(T) = 0,$$

where ${}_tD^{\alpha}_{t_f}$ is right RLFD. Employing Theorem 2.1 gives Eq (4.8) in the right CFD of fractional order α, and after applying Lemma 2.1 the adjoint equations (4.5) are satisfied.

For optimality conditions,

$$
\begin{aligned}
0 &= \frac{\partial H(\mathcal{S}^*, \mathcal{P}^*, \mathcal{L}^*, \mathcal{I}^*, \mathcal{R}^*, u_1^*, u_2^*, P, t)}{\partial u_1^*} = (p_1(t) - p_2(t))d_1^{\alpha}\mathcal{S}^*(t) - C_1u_1^*(t),\\
0 &= \frac{\partial H(\mathcal{S}^*, \mathcal{P}^*, \mathcal{L}^*, \mathcal{I}^*, \mathcal{R}^*, u_1^*, u_2^*, P, t)}{\partial u_2^*} = (p_3(t) - p_5(t))d_2^{\alpha}\mathcal{L}^*(t) + (p_4(t) - p_5(t))d_2^{\alpha}\mathcal{I}^*(t) - C_2u_2^*(t).
\end{aligned}
$$

Applying the upper and lower bounds for the controls u_1 and u_2, the optimal value of the objective functional $J(u_1, u_2)$ is acquired. This completes the proof of NOCs.

5. Simulation results of two-stage infection

The impact of u_1 and u_2 controls, by solving FOCP numerically, is investigated. In fact, there are two fundamental approaches to solving FOCPs: direct and indirect approaches. In direct methods, the FOCP is discretized and transformed into a nonlinear programming problem as illustrated in references [51, 52], but indirect methods are based on PMP so they are considered more suitable [53, 54]. In order to implement the indirect approach, it is necessary to derive the co-state, optimum controls, and all transversality constraints (such as those described in Theorem 4.1). Subsequently, a numerical scheme known as FBSM is constructed. The FBSM has many applications in the treatment of FOCPs, as evidenced by the literature [26, 27, 30, 55]. Herein, a brief outline of the procedures for implementing this method through the following algorithm:

Step 0 Begin the process by inputting ICs, parameter values, and an initial value of u_k; $k = 1, 2$ for $I = [0, T]$.

Step 1 Partition I into N subintervals, where the step-size $h = \frac{T}{N}$, $t_j = jh$, $j = 0, 1, ..., N$.

Step 2 Utilize current values of u_k with the given ICs

$$u_1(t_j) = \min\Big\{\max\Big\{0, \frac{(p_1(t_j) - p_2(t_j))d_1^{\alpha}\mathcal{S}(t_j)}{C_1}\Big\}, 1\Big\}, \quad j = 0, 1, ..., N,$$

$$u_2(t_j) = \min\Big\{\max\Big\{0, \frac{(p_3(t_j)-p_5(t_j))d_2^\alpha \mathcal{L}(t_j) + (p_4(t_j)-p_5(t_j))d_2^\alpha \mathcal{I}(t_j)}{C_2}\Big\}, 1\Big\},$$

in order to solve Eq (3.1) as a forward approach.

$$\begin{aligned}
\mathcal{S}(t_k) &= \mathcal{S}_0 + \tfrac{h^\alpha}{\Gamma(\alpha+1)}\sum_{j=0}^{k-1}\Theta_{j,k}\Big[\Lambda^\alpha\,(K-\mathcal{N}) - \Big(\beta^\alpha\frac{\mathcal{I}(t_j)}{K} + \epsilon\beta^\alpha\frac{\mathcal{L}(t_j)}{K}\Big)\mathcal{S}(t_j) - (\zeta^\alpha + d_1^\alpha u_1(t_j))\mathcal{S}(t_j) + \delta^\alpha\mathcal{P}(t_j)\Big],\\
\mathcal{P}(t_k) &= \mathcal{P}_0 + \frac{h^\alpha}{\Gamma(\alpha+1)}\sum_{j=0}^{k-1}\Theta_{j,k}\Big[d_1^\alpha u_1(t_j)\mathcal{S}(t_j) - (\delta^\alpha+\zeta^\alpha)\mathcal{P}(t_j)\Big],\\
\mathcal{L}(t_k) &= \mathcal{L}_0 + \frac{h^\alpha}{\Gamma(\alpha+1)}\sum_{j=0}^{k-1}\Theta_{j,k}\Big[\Big(\beta^\alpha\frac{\mathcal{I}(t_j)}{K} + \epsilon\beta^\alpha\frac{\mathcal{L}(t_j)}{K}\Big)\mathcal{S}(t_j) - (\zeta^\alpha+\rho^\alpha+\mu^\alpha+d_2^\alpha u_2(t_j))\mathcal{L}(t_j)\Big],\\
\mathcal{I}(t_k) &= \mathcal{I}_0 + \frac{h^\alpha}{\Gamma(\alpha+1)}\sum_{j=0}^{k-1}\Theta_{j,k}\Big[\mu^\alpha\mathcal{L}(t_j) - (\zeta^\alpha+\rho^\alpha+\psi^\alpha+d_2^\alpha u_2(t_j))\mathcal{I}(t_j)\Big],\\
\mathcal{R}(t_k) &= \mathcal{R}_0 + \frac{h^\alpha}{\Gamma(\alpha+1)}\sum_{j=0}^{k-1}\Theta_{j,k}\Big[(\psi^\alpha+d_2^\alpha u_2(t_j))\mathcal{I}(t_j) - (\zeta^\alpha+\gamma^\alpha)\mathcal{R}(t_j) + d_2^\alpha u_2(t_j)\mathcal{L}(t_j)\Big],
\end{aligned}$$

for $k = 1, 2, ..., N$, where

$$\Theta_{j,k} = (k-j)^\alpha - (k-j-1)^\alpha. \tag{5.1}$$

Step 3 Employ the values of u_k, terminal condition (4.6), and $\mathcal{S}, \mathcal{P}, \mathcal{L}, \mathcal{I}$, and $\mathcal{R}$ to get the solution of adjoint system (4.5) as a backward approach. For $\vartheta = t^*_{N-j}$, leading to

$$\begin{aligned}
p_1(t^*_{N-k-1}) &= \frac{h^\alpha}{\Gamma(\alpha+1)}\sum_{j=0}^{k}\Theta_{j,k+1}\Big[\Big(p_3(\vartheta)-p_1(\vartheta)\Big)\Big(\beta^\alpha\frac{\mathcal{I}(\vartheta)}{K} + \epsilon\beta^\alpha\frac{\mathcal{L}(\vartheta)}{K}\Big) + d_1^\alpha u_1(\vartheta)\\
&\times \Big(p_2(\vartheta)-p_1(\vartheta)\Big) - \zeta^\alpha p_1(\vartheta)\Big],\\
p_2(t^*_{N-k-1}) &= \frac{h^\alpha}{\Gamma(\alpha+1)}\sum_{j=0}^{k}\Theta_{j,k+1}\Big[\delta^\alpha\Big(p_1(\vartheta)-p_2(\vartheta)\Big) - \zeta^\alpha p_2(\vartheta)\Big],\\
p_3(t^*_{N-k-1}) &= \frac{h^\alpha}{\Gamma(\alpha+1)}\sum_{j=0}^{k}\Theta_{j,k+1}\Big[A_2 + \epsilon\beta^\alpha\frac{\mathcal{S}(\vartheta)}{K}\Big(p_3(\vartheta)-p_1(\vartheta)\Big) + \mu^\alpha\Big(p_4(\vartheta)-p_3(\vartheta)\Big)\\
&+ d_2^\alpha u_2(\vartheta)\Big(p_5(\vartheta)-p_3(\vartheta)\Big) - (\zeta^\alpha+\rho^\alpha)p_3(\vartheta)\Big],\\
p_4(t^*_{N-k-1}) &= \frac{h^\alpha}{\Gamma(\alpha+1)}\sum_{j=0}^{k}\Theta_{j,k+1}\Big[A_1 + \beta^\alpha\frac{\mathcal{S}(\vartheta)}{K}\Big(p_3(\vartheta)-p_1(\vartheta)\Big) + (\psi^\alpha+d_2^\alpha u_2(\vartheta))\\
&\times \Big(p_5(\vartheta)-p_4(\vartheta)\Big) - (\zeta^\alpha+\rho^\alpha)p_4(\vartheta)\Big],\\
p_5(t^*_{N-k-1}) &= \frac{h^\alpha}{\Gamma(\alpha+1)}\sum_{j=0}^{k}\Theta_{j,k+1}\Big[-(\zeta^\alpha+\gamma^\alpha)p_5(\vartheta)\Big],
\end{aligned}$$

Step 4 Update the controls values u_k by incorporating the obtained values of $\mathcal{S}, \mathcal{P}, \mathcal{L}, \mathcal{I}, \mathcal{R}$ (***Step 2***) and p_1, p_2, p_3, p_4, p_5 (***Step 3***) in Eq (4.7).

Step 5 Evaluate convergence: if the differences between values of state and adjoint variables at the current and previous iteration are very small amounts, it means that the required results have been given and stopped the iteration. Otherwise, go back to ***Step 2*** to continue the process.

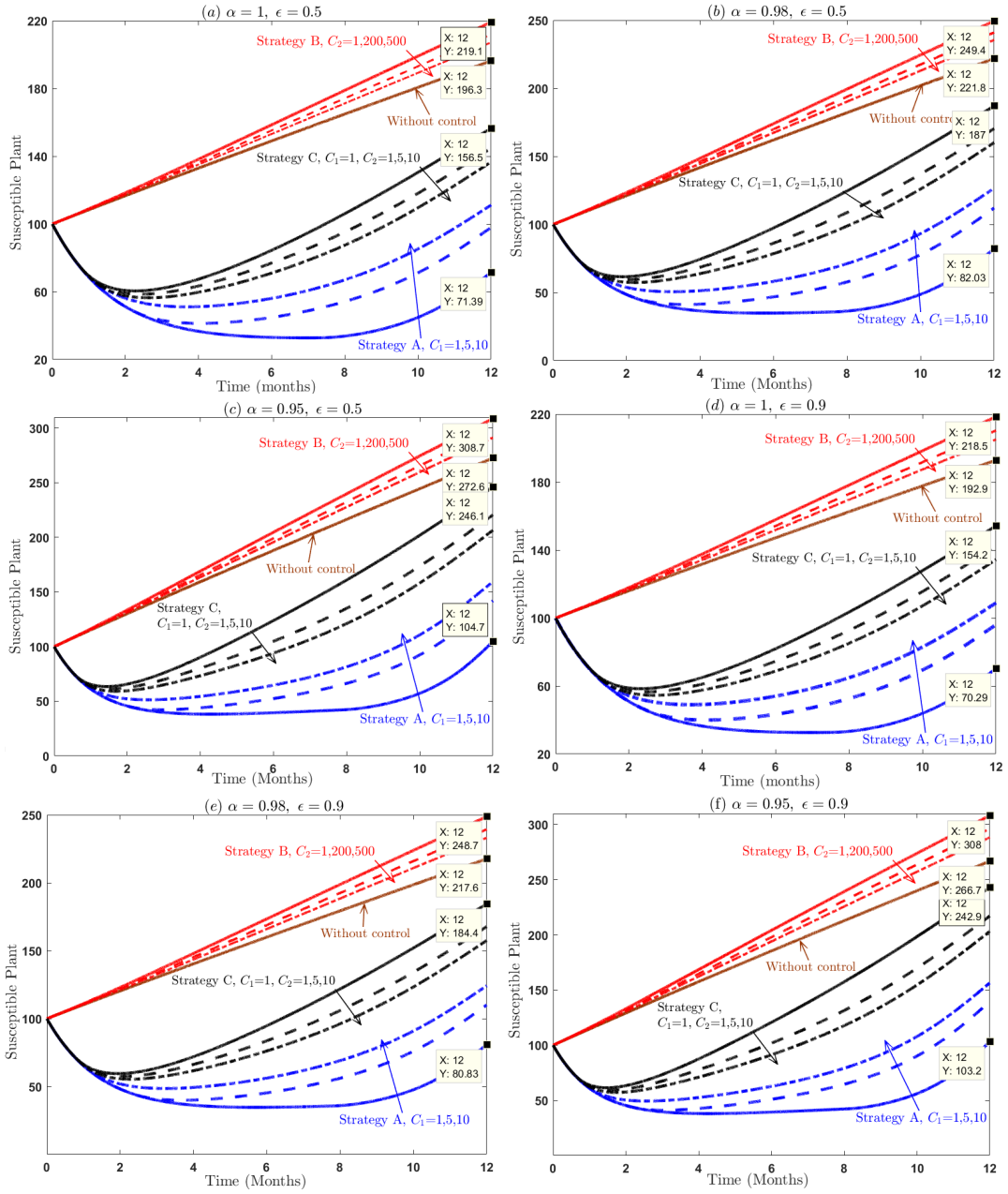

Figure 3. Dynamical behavior of $\mathcal{S}(t)$ without and with control strategies (in Strategy **A**: $C_1 = 1, 5, 10$, in Strategy **B**: $C_2 = 1, 200, 500$, and in Strategy **C**: $C_1 = 1, C_2 = 1, 5, 10$) where sub-figures (a)–(c) at $\epsilon = 0.5$ and sub-figures (d)–(f) at $\epsilon = 0.9$ with $\alpha = 1, 0.98, 0.95$.

Therefore, numerical simulations are presented in the following figures to display the influence of curative (u_1) and preventive (u_2) control measures on the behavior of the FOM (3.1). Moreover, the effect of the transmission factor ϵ on this two-stage plant disease model is examined, along with the influence of α on the proposed model. To proceed, the convenient parameter values provided in Table 2 and ICs in Table 1 are employed, with weight values $A_1 = A_2 = 1$. The control weight values are presented in the figures, where variations in C_1 and C_2 influence the optimal solution of this FOM. The findings are summarized in the following strategies.

Strategy **A** (Blue lines): Using only preventive treatment control (i.e., $u_1 \neq 0$ and $u_2 = 0$).

Strategy **B** (Red lines): Using only a curative treatment control (i.e., $u_2 \neq 0$ and $u_1 = 0$).

Strategy **C** (Black lines): Using the incorporation of preventive and curative controls (i.e., $u_1, u_2 \neq 0$).

The next figures compare the effects of the proposed control strategies with uncontrolled cases on the FOCP results (4.1). In addition, the impact of ϵ and α on the behavior of solutions for plant compartments is explained.

Figure 3(a),(d) shows the behavior of the three suggested strategies on $\mathcal{S}(t)$ when $\alpha = 1$ with various values of weight factors at $\epsilon = 0.5$ and $\epsilon = 0.9$. In the rest of the sub-figures in Figure 3, the impact of α with the presence of controls and in their absence at the two values of ϵ and various weight factors is presented. Note that $\mathcal{S}(t)$ is generally sensitive to changes in the parameter ϵ in the case without control, but when the controls are active the effect of ϵ on it is very weak because the controls suppress the disease.

Figures 4 and 5 display the influence of the strategies **A**, **B** and **C** on $\mathcal{I}(t)$ and $\mathcal{L}(t)$. Sub-figures 4(a),(d) and 5(a),(d) present the influence of varying ϵ and weight factors when $\alpha = 1$. In the remaining sub-figures, the effect of α on the behavior of the solution is demonstrated. Observe that all strategies are effective in reducing infected plants, but Strategy **C** is the best in terms of controlling disease. Also note that increasing the value of ϵ does not have a significant effect in the case of the presence of controls, because the PDT is controlled.

In Figure 6, the control behavior of each strategy is shown (where $C_1 = C_2 = 1$), taking into account the effect of α. It is observed that the maximum efforts of u_1 and u_2 controls decrease when $\alpha \to 1$ (e.g., $\alpha = 0.98, 0.95$). Moreover, as evident in Figure 6(d)–(f), all strategies when $\epsilon = 0.9$ require that the efforts of u_1 and u_2 must kept at the maximum for longer in the control period time when compared to the case $\epsilon = 0.5$ as in Figure 6(a)–(c). This observation confirms the critical impact of ϵ on the dynamics of control measures u_1 and u_2 for the proposed strategies.

From Figure 7, depicting R_c yields confirmation that the distinguishing factor ϵ belongs to the interval $(0, 1)$ for several reasons. Notably, if $\epsilon = 1$, this means that $\mathcal{L}(t)$ transmits the disease at the same rate of infection as $\mathcal{I}(t)$, resulting in R_c, and (3.14) in this case is imaginary value. This characteristic is the main reason for choosing $\epsilon \in (0, 1)$. Further insights can be drawn from Figure 7, specifically at $\epsilon = 0.9$, where a noticeable and rapid decrease in R_c is observed when α takes values of 0.98 and 0.95, compared to the case when $\alpha = 1$.

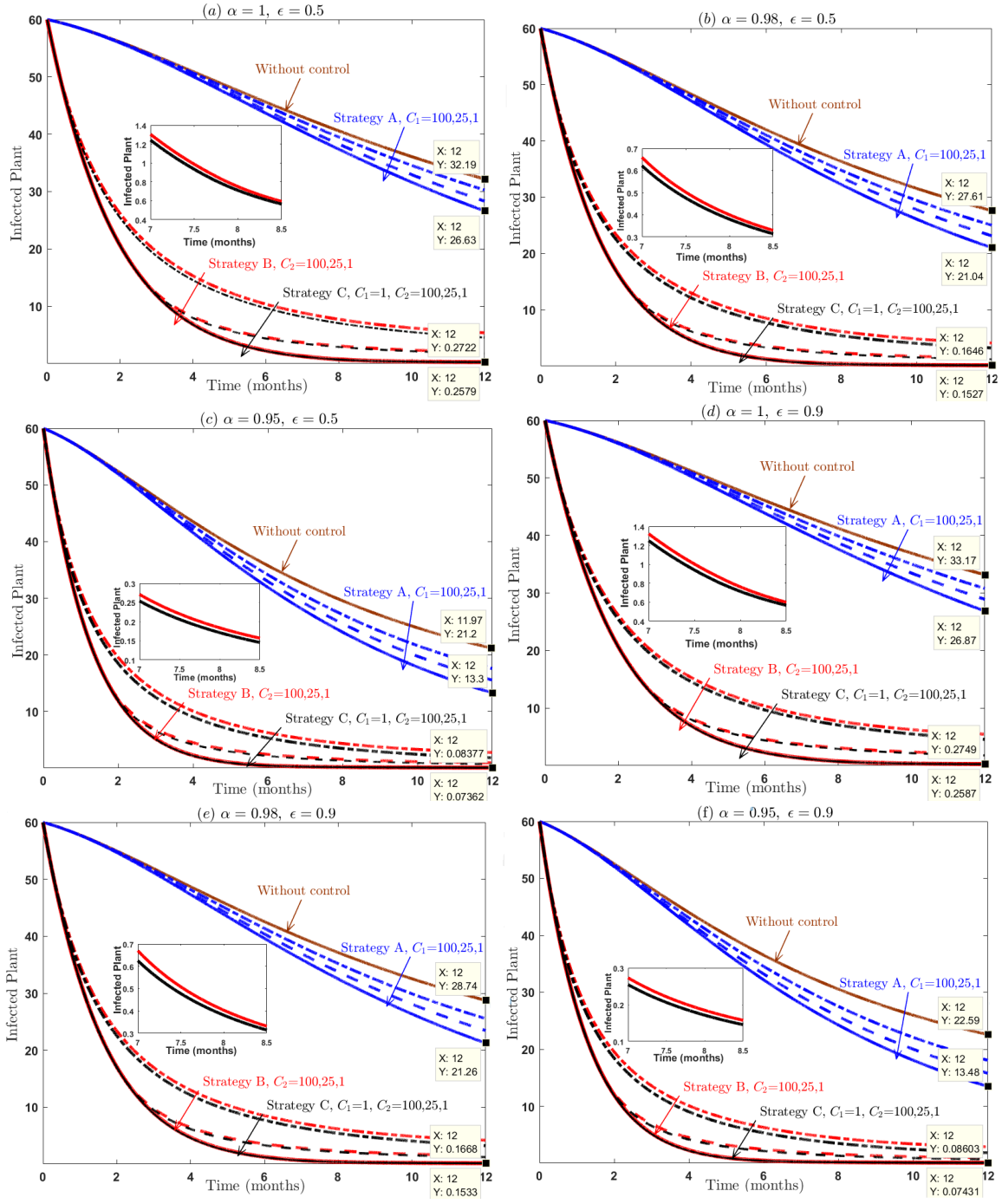

Figure 4. Dynamical behavior of $\mathcal{I}(t)$ without and with control strategies (in Strategy **A**: $C_1 = 1, 25, 100$, in Strategy **B**: $C_2 = 1, 25, 100$, and in Strategy **C**: $C_1 = 1, C_2 = 1, 25, 100$) where sub-figures (a)–(c) at $\epsilon = 0.5$ and sub-figures (d)–(f) at $\epsilon = 0.9$ with $\alpha = 1, 0.98, 0.95$.

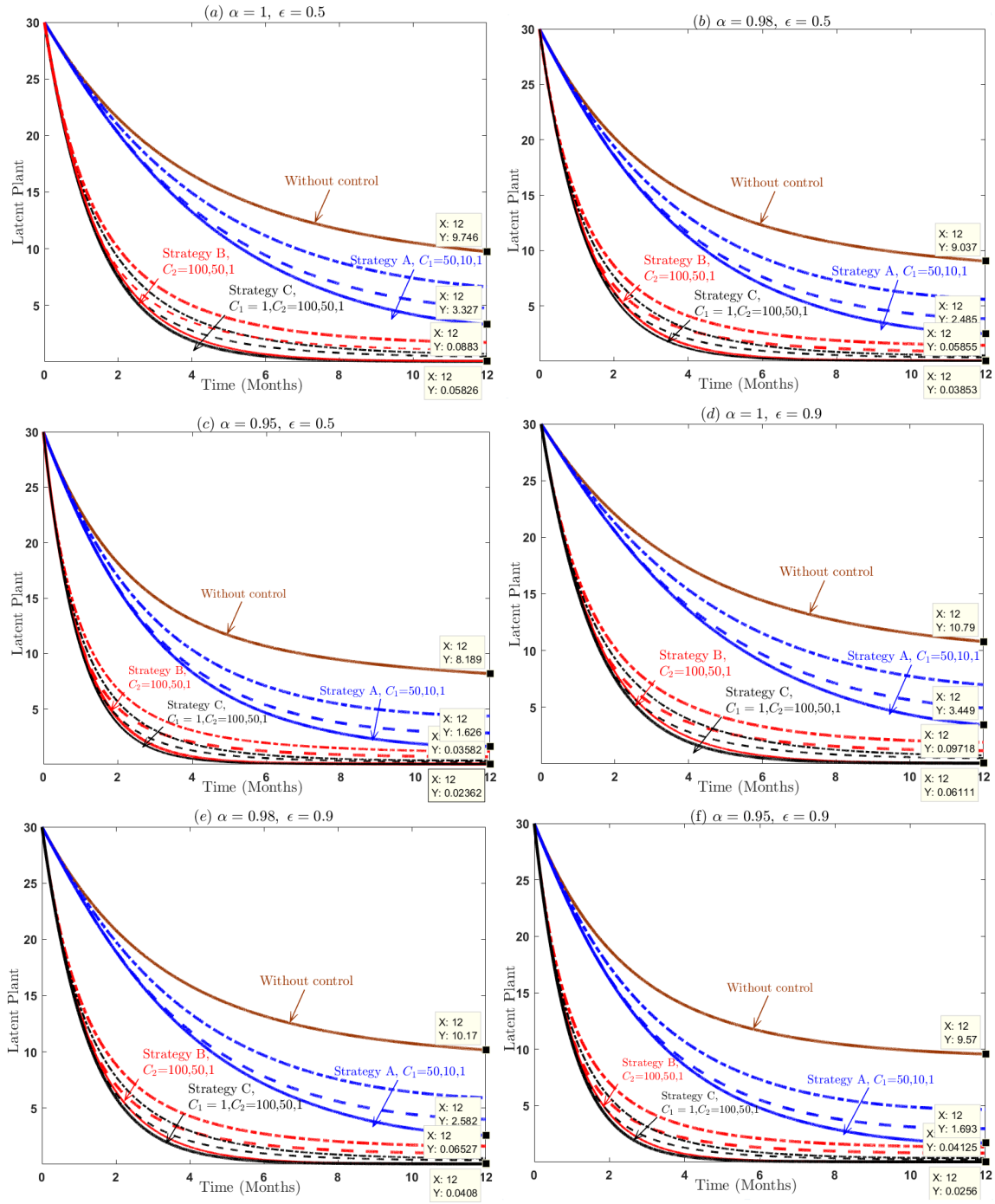

Figure 5. Dynamical behavior of $\mathcal{L}(t)$ without and with control strategies (in Strategy **A**: $C_1 = 1, 10, 50$, in Strategy **B**: $C_2 = 1, 50, 100$, and in Strategy **C**: $C_1 = 1, C_2 = 1, 50, 100$) where sub-figures (a)–(c) at $\epsilon = 0.5$ and sub-figures (d)–(f) at $\epsilon = 0.9$ with $\alpha = 1, 0.98, 0.95$.

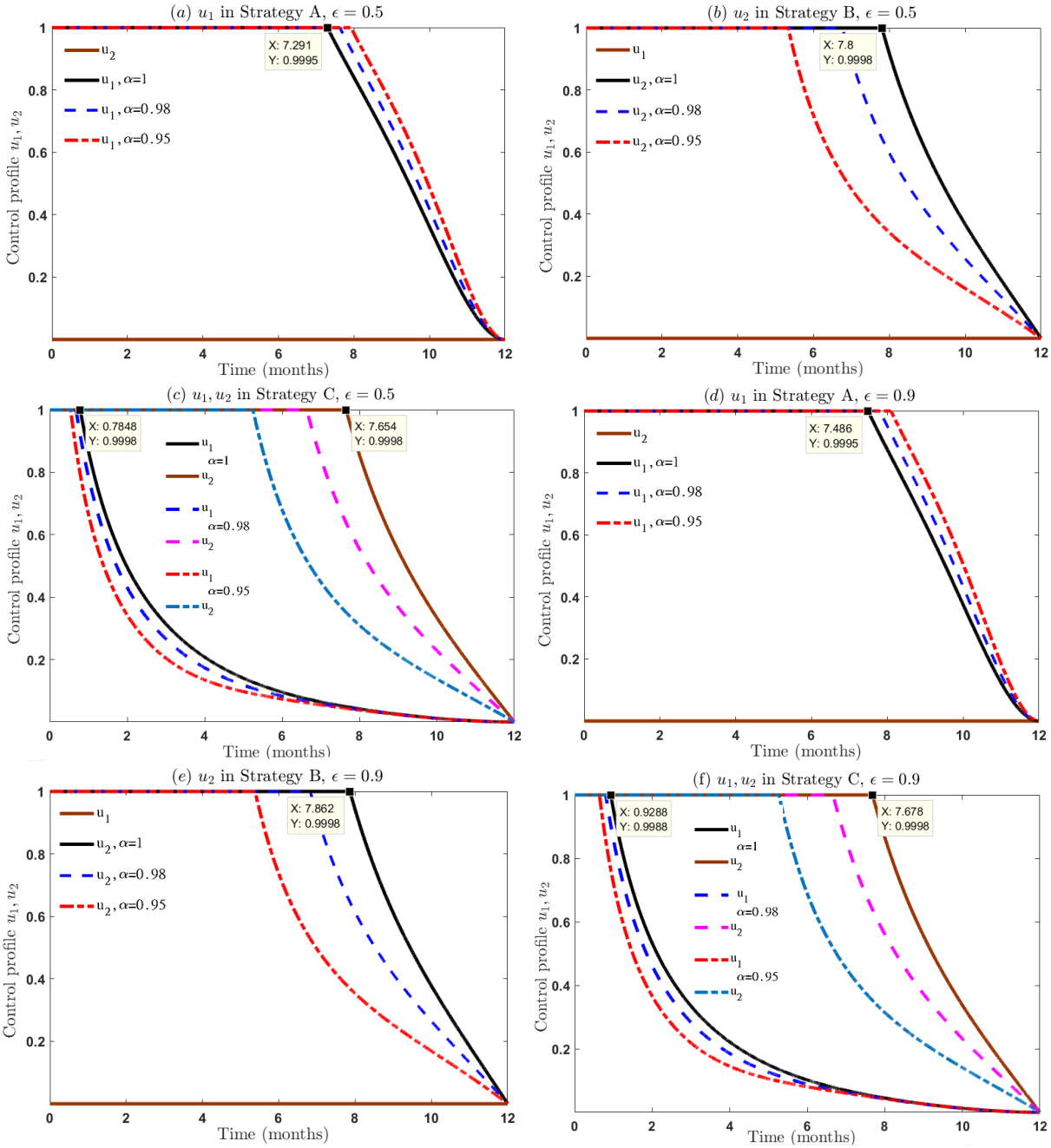

Figure 6. Controls profile in all strategies: (a) behavior of u_1 with $C_1 = 1$ (Strategy **A**), (b) behavior of u_2 with $C_2 = 1$ (Strategy **B**), (c) behavior of u_1, u_2 with $C_1 = C_2 = 1$ (Strategy **C**) for $\epsilon = 0.5$ and (d) behavior of u_1 with $C_1 = 1$ (Strategy **A**), (e) behavior of u_2 with $C_2 = 1$ (Strategy **B**), (f) behavior of u_1, u_2 with $C_1 = C_2 = 1$ (Strategy **C**) for $\epsilon = 0.9$ with $\alpha = 1, 0.98, 0.95$.

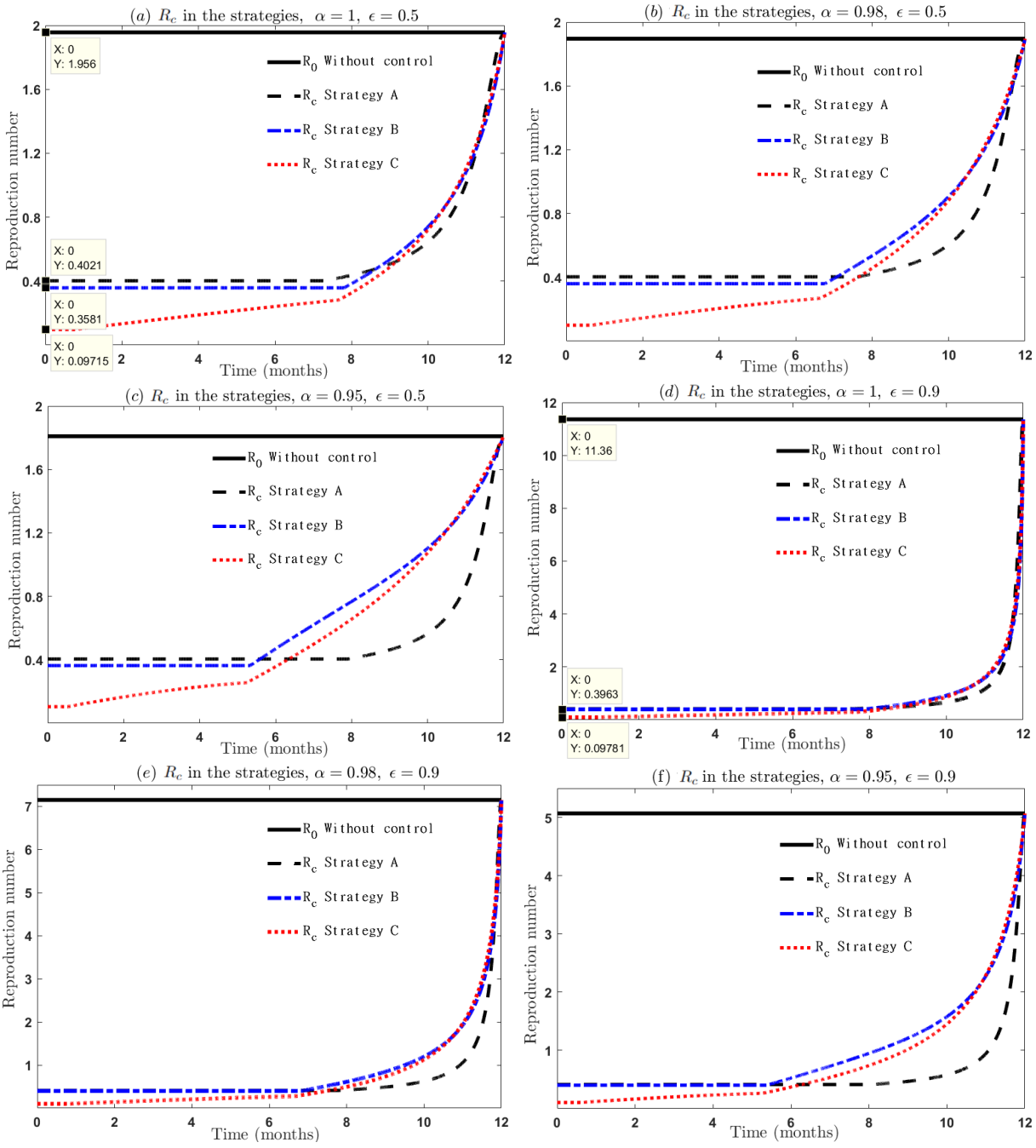

Figure 7. Behavior of R_0 (without control), R_c in all strategies where (a) $\alpha = 1$, (b) $\alpha = 0.98$, (c) $\alpha = 0.95$ for $\epsilon = 0.5$, (d) $\alpha = 1$, (e) $\alpha = 0.98$, and (f) $\alpha = 0.95$ for $\epsilon = 0.9$.

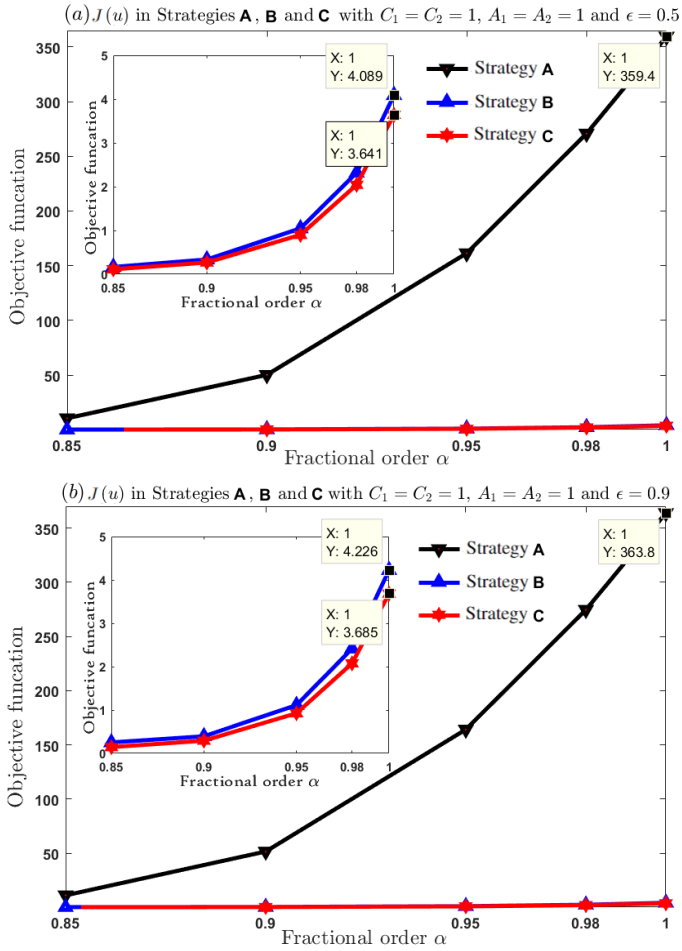

Figure 8. Objective function versus $\alpha = 0.85, 0.9, 0.95, 0.98, 1$, where (a) $J(u_1^*, u_2^*)$ in Strategies **A**, **B**, and **C** with $C_1 = C_2 = 1, A_1 = A_2 = 1$, and $\epsilon = 0.5$, (b) $J(u_1^*, u_2^*)$ in Strategies **A**, **B**, and **C** with $C_1 = C_2 = 1, A_1 = A_2 = 1$, and $\epsilon = 0.9$.

Figure 8 illustrates the influence of α on $J(u_1, u_2)$ for all control strategies. Significantly, $J(u_1, u_2)$ shows a steady decrease when α is less than 1. The findings in Table 3 include the values of $J(u_1, u_2)$ and $\mathcal{I}(T) + \mathcal{L}(T)$ at the final time, for varying values of α in each strategy, also encompassing the uncontrolled case. Furthermore, in Strategy **C**, the values of $J(u_1, u_2)$ and $\mathcal{I}(T) + \mathcal{L}(T)$ are lower compared to Strategies **A** and **B** for the different values of α. Additionally, in all strategies, the values of $J(u_1, u_2)$ and $\mathcal{I}(T) + \mathcal{L}(T)$ consistently decrease when α values are less than one, highlighting the distinguishable effect of fractional order.

Table 3. Comparison of $J(u_1^*, u_2^*)$ and $\mathcal{I}(T) + \mathcal{L}(T)$ for all presented control strategies.

α	Strategy **A**				Strategy **B**				Strategy **C**				Uncontrolled case			
	J		$\mathcal{I}+\mathcal{L}$		J		$\mathcal{I}+\mathcal{L}$		J		$\mathcal{I}+\mathcal{L}$		J		$\mathcal{I}+\mathcal{L}$	
	$\epsilon=0.5$	$\epsilon=0.9$	$\epsilon=0.5$	$\epsilon=0.9$	$\epsilon=0.5$	$\epsilon=0.9$	$\epsilon=0.5$	$\epsilon=0.9$	$\epsilon=0.5$	$\epsilon=0.9$	$\epsilon=0.5$	$\epsilon=0.9$	$\epsilon=0.5$	$\epsilon=0.9$	$\epsilon=0.5$	$\epsilon=0.9$
1	359.435	363.813	29.953	30.318	4.089	4.226	0.341	0.352	3.641	3.685	0.303	0.308	503.194	527.487	41.933	43.957
0.98	270.816	274.517	23.521	23.843	2.319	2.414	0.201	0.211	2.042	2.074	0.177	0.180	421.903	448.042	36.644	38.914
0.95	161.406	164.102	14.924	15.173	1.047	1.113	0.097	0.103	0.899	0.925	0.083	0.086	317.340	347.779	29.341	32.155

6. Conclusions

This article developed and analyzed a FOM to understand and control PDT within a two-stage infection mathematical framework. The well-posedness of the model by proving the existence, uniqueness, nonnegativity, and boundedness of solutions was established. The R_c was derived and shown to determine the local and global stability of both the DFE point and EEP. Sensitivity analysis identified the parameters with the most significant direct and inverse influence on R_c, as presented in Figure 2, highlighting key targets for intervention. Moreover, a FOCP was constructed to minimize disease prevalence by applying two control measures: preventive treatment and curative treatment. Using a kind of PMP, the fractional necessary optimality conditions were derived in order to solve this FOCP numerically, provide appropriate explanations for the proposed strategies, compare them, and identify the most effective one in reducing the disease. Numerical simulations, solved via an FBSM based on the fractional Euler method, demonstrated the substantial efficacy of these controls in reducing the infected plant population, as shown in Figures 3–7. The simulations also revealed the significant impact of the ϵ in addition to α, which incorporates memory effects, offering a novel perspective on how past epidemiological states influence future disease dynamics. Also, the elimination of the plant infection can be established through the suggested strategies, a crucial insight for plant epidemiology. While the model provides valuable theoretical insights, its applicability is subject to several limitations.

A fundamental limitation is the lack of direct comparison of the numerical results with real-world epidemiological field data. This is primarily due to the practical difficulty in obtaining comprehensive, accurate longitudinal datasets for plant disease transmission that precisely measure the model's state variables (e.g., latent and infected plants) and parameters (e.g., transmission, progression, and mortality rates) over time. This constraint limits the direct empirical validation of the model.

Future work may extend the model with delays, stochasticity, alternative fractional operators, or incorporate additional variables, besides proposing new effective control measures. Also, future work must urgently focus on bridging the gap between theoretical results and real-world data by seeking out the datasets necessary for this.

Use of AI tools declaration

The authors declare they have not used Artificial Intelligence (AI) tools in the creation of this article.

Acknowledgments

The authors are thankful to the Deanship of Graduate Studies and Scientific Research at the University of Bisha for supporting this work through the Fast-Track Research Support Program.

Conflict of interest

The authors declare no conflicts of interest in this paper.

References

1. J. B. Ristaino, P. K. Anderson, D. P. Bebber, K. A. Brauman, N. J. Cunniffe, N. V. Fedoroff, et al., The persistent threat of emerging plant disease pandemics to global food security, *Proc. Natl. Acad. Sci. U.S.A.*, **118** (2021), e2022239118. https://doi.org/10.1073/pnas.2022239118
2. D. M. Rizzo, M. Lichtveld, J. A. K. Mazet, E. Togami, S. A. Miller, Plant health and its effects on food safety and security in a One Health framework: Four case studies, *One Health Outlook*, **3** (2021), 1–9. https://doi.org/10.1186/s42522-021-00038-7
3. X. Zhang, X. Dong, Life-or-death decisions in plant immunity, *Curr. Opin. Immunol.*, **75** (2022), 102169. https://doi.org/10.1016/j.coi.2022.102169
4. S. Hou, Y. Yang, D. Wu, C. Zhang, Plant immunity: Evolutionary insights from PBS1, Pto, and RIN4, *Plant Signaling Behav.*, **6** (2011), 794–799. https://doi.org/10.4161/psb.6.6.15143
5. M. S. Sisterson, D. C. Stenger, Roguing with replacement in perennial crops: Conditions for successful disease management, *Phytopathology*, **103** (2013), 117–128. https://doi.org/10.1094/PHYTO-05-12-0101-R
6. F. Nakasuji, S. Miyai, V. Kawamoto, K. Kiritani, Mathematical epidemiology of rice dwarf virus transmitted by green rice leafhoppers: A differential equation model, *J. Appl. Ecol.*, **22** (1985), 839–847. https://doi.org/10.2307/2403233
7. N. Anggriani, N. Istifadah, M. Hanifah, A. Supriatna, A mathematical model of protectant and curative fungicide application and its stability analysis, *IOP Conf. Ser.: Earth Environ. Sci.*, **31** (2016), 012014. https://doi.org/10.1088/1755-1315/31/1/012014
8. N. Anggriani, M. Ndii, D. Arumi, N. Istifadah, A. Supriatna, Mathematical model for plant disease dynamics with curative and preventive treatments, *AIP Conf. Proc.*, **2043** (2018), 020016. https://doi.org/10.1063/1.5080035
9. N. Anggriani, M. Ndii, N. Istifadah, A. Supriatna, Disease dynamics with curative and preventive treatments in a two-stage plant disease model, *AIP Conf. Proc.*, **2043** (2018), 020010. https://doi.org/10.1063/1.5080029
10. J. Van der Plank, *Plant Diseases: Epidemics and Control*, Academic Press, New York, 1963.
11. H. M. Ali, I. Ameen, Y. A. Gaber, The effect of curative and preventive optimal control measures on a fractional order plant disease model, *Math. Comput. Simul.*, **220** (2024), 496–515. https://doi.org/10.1016/j.matcom.2024.02.009
12. H. M. Srivastava, V. P. Dubey, R. Kumar, J. Singh, D. Kumar, D. Baleanu, An efficient computational approach for a fractional-order biological population model with carrying capacity, *Chaos Solitons Fractals*, **138** (2020), 109880. https://doi.org/10.1016/j.chaos.2020.109880
13. L. Frunzo, R. Garra, A. Giusti, V. Luongo, Modeling biological systems with an improved fractional Gompertz law, *Commun. Nonlinear Sci. Numer. Simul.*, **74** (2019), 260–267. https://doi.org/10.1016/j.cnsns.2019.03.024
14. J. Singh, D. Kumar, Z. Hammouch, A. Atangana, A fractional epidemiological model for computer viruses pertaining to a new fractional derivative, *Appl. Math. Comput.*, **316** (2018), 504–515. https://doi.org/10.1016/j.amc.2017.08.048

15. S. Maiti, S. Shaw, G. C. Shit, Caputo-Fabrizio fractional order model on MHD blood flow with heat and mass transfer through a porous vessel in the presence of thermal radiation, *Physica A*, **540** (2020), 123149. https://doi.org/10.1016/j.physa.2019.123149

16. S. Chakraverty, R. M. Jena, S. K. Jena, *Computational Fractional Dynamical Systems: Fractional Differential Equations and Applications*, John Wiley & Sons, 2022.

17. V. E. Tarasov, Non-linear macroeconomic models of growth with memory, *Mathematics*, **8** (2020), 2078. https://doi.org/10.3390/math8112078

18. V. E. Tarasov, No nonlocality, no fractional derivative, *Commun. Nonlinear Sci. Numer. Simul.*, **62** (2018), 157–163. https://doi.org/10.1016/j.cnsns.2018.02.019

19. W. Gao, X. Tian, R. Shi, Dynamic analysis and optimal control of a fractional order predator-prey model with economic threshold, *Electron. Res. Arch.*, **33** (2025), 4529–4558. https://doi.org/10.3934/era.2025205

20. A. Jan, S. Boulaaras, F. A. Abdullah, R. Jan, Dynamical analysis, infections in plants, and preventive policies utilizing the theory of fractional calculus, *Eur. Phys. J. Spec. Top.*, **232** (2023), 2497–2512. https://doi.org/10.1140/epjs/s11734-023-00926-1

21. Q. Dai, L. Guo, Modeling and optimal control analysis of age-structured Brucellosis under environmental transmission with vaccination and culling, *Electron. Res. Arch.*, **33** (2025), 5100–5132. https://doi.org/10.3934/era.2025229

22. R. Alharbi, R. Jan, S. Alyobi, Y. Altayeb, Z. Khan, Mathematical modeling and stability analysis of the dynamics of monkeypox via fractional-calculus, *Fractals*, **30** (2022), 2240266. https://doi.org/10.1142/S0218348X22402666

23. A. Coronel, F. Huancas, C. Isoton, A. Tello, Optimal control problem and reaction identification term for carrier-borne epidemic spread with a general infection force and diffusion, *Electron. Res. Arch.*, **33** (2025), 4435–4467. https://doi.org/10.3934/era.2025202

24. R. Mukhtar, C. Y. Chang, M. A. Z. Raja, N. I. Chaudhary, C. M. Shu, Novel nonlinear fractional order Parkinson's disease model for brain electrical activity rhythms: Intelligent adaptive Bayesian networks, *Chaos Solitons Fractals*, **180** (2024), 114557. https://doi.org/10.1016/j.chaos.2024.114557

25. L. S. Pontryagin, *The Mathematical Theory of Optimal Processes*, Gordon and Breach Science Publishers, 1986.

26. I. Ameen, D. Baleanu, H. M. Ali, Different strategies to confront maize streak disease based on fractional optimal control formulation, *Chaos Solitons Fractals*, **164** (2022), 112699. https://doi.org/10.1016/j.chaos.2022.112699

27. H. M. Ali, I. Ameen, Stability and optimal control analysis for studying the transmission dynamics of a fractional-order MSV epidemic model, *J. Comput. Appl. Math.*, **434** (2023), 115352. https://doi.org/10.1016/j.cam.2023.115352

28. H. M. Ali, I. Ameen, Save the pine forests of wilt disease using a fractional optimal control strategy, *Chaos Solitons Fractals*, **132** (2020), 109554. https://doi.org/10.1016/j.chaos.2019.109554

29. R. Jan, N. N. A. Razak, S. Boulaaras, Z. U. Rehman, S. Bahramand, Mathematical analysis of the transmission dynamics of viral infection with effective control policies via fractional derivative, *Nonlinear Eng.*, **12** (2023), 20220342. https://doi.org/10.1515/nleng-2022-0342
30. H. M. Ali, I. Ameen, Optimal control strategies of a fractional-order model for Zika virus infection involving various transmissions, *Chaos Solitons Fractals*, **146** (2021), 110864. https://doi.org/10.1016/j.chaos.2021.110864
31. I. Ameen, D. Baleanu, H. M. Ali, An efficient algorithm for solving the fractional optimal control of SIRV epidemic model with a combination of vaccination and treatment, *Chaos Solitons Fractals*, **137** (2020), 109892. https://doi.org/10.1016/j.chaos.2020.109892
32. A. M. A. El-Sayed, S. Z. Rida, Y. A. Gaber, Dynamical of curative and preventive treatments in a two-stage plant disease model of fractional order, *Chaos Solitons Fractals*, **137** (2020), 109879. https://doi.org/10.1016/j.chaos.2020.109879
33. I. Podlubny, *Fractional Differential Equations, Mathematics in Science and Engineering*, Academic Press, San Diego, CA, 1999.
34. D. Baleanu, K. Diethelm, E. Scalas, J. J. Trujillo, *Fractional Calculus: Models and Numerical Methods, Series on Complexity, Nonlinearity and Chaos*, World Scientific, 2012.
35. I. Ameen, M. Hidan, Z. Mostefaoui, H. M. Ali, Fractional optimal control with fish consumption to prevent the risk of coronary heart disease, *Complexity*, **2020** (2020), 9823753. https://doi.org/10.1155/2020/9823753
36. K. Diethelm, *The Analysis of Fractional Differential Equations: An Application-Oriented Exposition Using Operators of Caputo Type*, Springer, 2010. https://doi.org/10.1007/978-3-642-14574-2
37. V. Dafardar-Gejji, *Fractional Calculus and Fractional Differential Equations*, Springer, 2019. https://doi.org/10.1007/978-981-13-9227-6
38. M. S. Tavazoei, M. Haeri, Chaotic attractors in incommensurate fractional order systems, *Physica D*, **237** (2008), 2628–2637. https://doi.org/10.1016/j.physd.2008.03.037
39. N. Anggriani, D. Arumi, E. Hertini, N. Istifadah, A. Supriatna, Dynamical analysis of plant disease model with roguing, replanting and preventive treatment, in *4th ICRIEMS proceedings 978-602-74529-2-3*, The Faculty Of Mathematics And Natural Sciences, Yogyakarta State University, 2017.
40. M. S. Chan, M. J. Jeger, An analytical model of plant virus disease dynamics with roguing and replanting, *J. Appl. Ecol.*, **31** (1994), 413–427. https://doi.org/10.2307/2404439
41. E. Venturino, P. K. Roy, F. Al Basir, A. Datta, A model for the control of the mosaic virus disease in jatropha curcas plantations, *Energy Ecol. Environ.*, **1** (2016), 360–369. https://doi.org/10.1007/s40974-016-0033-8
42. T. Sardar, S. Rana, S. Bhattacharya, K. Al-khaled, J. Chattopadhya, A generic model for a single strain mosquito-transmitted disease with memory on the host and the vector, *Math. Biosci.*, **2015** (2015), 18–36. https://doi.org/10.1016/j.mbs.2015.01.009
43. O. Diekmann, J. A. P. Heesterbeek, M. G. Roberts, The construction of next-generation matrices for compartmental epidemic models, *J. R. Soc. Interface*, **7** (2010), 873–885. https://doi.org/10.1098/rsif.2009.0386

44. P. van den Driessche, J. Watmough, Reproduction numbers and sub-threshold endemic equilibria for compartmental models of disease transmission, *Math. Biosci.*, **180** (2002), 29–48. https://doi.org/10.1016/S0025-5564(02)00108-6

45. G. J. Olsder, J. W. van der Woude, *Mathematical Systems Theory*, third edition, VSSD, 2005.

46. J. P. C. dos Santos, E. Monteiro, G. B. Vieira, Global stability of fractional SIR epidemic model, *Proc. Ser. Braz. Soc. Appl. Comput. Math.*, **5** (2017), 1–7. https://doi.org/10.5540/03.2017.005.01.0019

47. J. Huo, H. Zhao, L. Zhu, The effect of vaccines on backward bifurcation in a fractional order HIV model, *Nonlinear Anal. Real World Appl.*, **26** (2015), 289–305. https://doi.org/10.1016/j.nonrwa.2015.05.014

48. N. Chitnis, J. M. Hyman, J. M. Cushing, Determining important parameters in the spread of malaria through the sensitivity analysis of a mathematical model, *Bull. Math. Biol.*, **70** (2008), 1272–1296. https://doi.org/10.1007/s11538-008-9299-0

49. S. A. Pedro, H. Rwezaura, J. M. Tchuenche, Time-varying sensitivity analysis of an influenza model with interventions, *Int. J. Biomath.*, **15** (2022), 2150098. https://doi.org/10.1142/S1793524521500984

50. H. M. Ali, F. L. Pereira, S. M. A. Gama, A new approach to the Pontryagin maximum principle for nonlinear fractional optimal control problems, *Math. Methods Appl. Sci.*, **39** (2016), 3640–3649. https://doi.org/10.1002/mma.3811

51. A. B. Salati, M. Shamsi, D. F. M. Torres, Direct transcription methods based on fractional integral approximation formulas for solving nonlinear fractional optimal control problems, *Commun. Nonlinear Sci. Numer. Simul.*, **67** (2019), 334–350. https://doi.org/10.1016/j.cnsns.2018.05.011

52. S. Nemati, P. M. Nemati, D. F. M. Torres, A numerical approach for solving fractional optimal control problems using modified hat functions, *Commun. Nonlinear Sci. Numer. Simul.*, **78** (2019), 104849. https://doi.org/10.1016/j.cnsns.2019.104849

53. M. S. Ali, M. K. Almoaeet, B. Albuohimad, An indirect spectral collocation method based on shifted Jacobi functions for solving some class of fractional optimal control problems, *J. Phys. Conf. Ser.*, **1818** (2021), 012129. https://doi.org/10.1088/1742-6596/1818/1/012129

54. P. Drag, K. Styczen, M. Kwiatkowska, A. Szczurek, A review on the direct and indirect methods for solving optimal control problems with differential-algebraic constraints, in *Recent Advances in Computational Optimization*, **610** (2016), 91–105. https://doi.org/10.1007/978-3-319-21133-6_6

55. H. Kheiri, M. Jafari, Stability analysis of a fractional order model for the HIV/AIDS epidemic in a patchy environment, *J. Comput. Appl. Math.*, **346** (2019), 323–339. https://doi.org/10.1016/j.cam.2018.06.055

Appendix

Verify the positivity of coefficients $\mathcal{A}_1, \mathcal{A}_2, \mathcal{A}_3, \mathcal{A}_4$ given in Eq (3.19) and holding the inequality $\mathcal{A}_1\mathcal{A}_2\mathcal{A}_3 > \mathcal{A}_3^2 + \mathcal{A}_1^2\mathcal{A}_4$.

Table A1. Numerical verification of stability conditions for the EEP Ξ_{eq}^{**}, when $R_c > 1$.

α	ϵ	R_c	A_1	$\mathcal{A}_2$	$\mathcal{A}_3$	$\mathcal{A}_4$	$\mathcal{A}_1\mathcal{A}_2\mathcal{A}_3$	$\mathcal{A}_3^2 + \mathcal{A}_1^2\mathcal{A}_4$
1	0.9	11.3622	0.3368	0.0199	7.0933e-04	2.0766e-05	4.7480e-06	2.8593e-06
1	0.5	1.9559	0.3643	0.0197	5.2276e-04	1.5184e-05	3.7586e-06	2.2889e-06
0.98	0.9	5.5925	0.3692	0.0246	9.8534e-04	3.2251e-05	8.9458e-06	5.3659e-06
0.98	0.5	1.8389	0.3992	0.0244	7.2470e-04	2.3500e-05	7.0595e-06	4.2700e-06
0.95	0.9	3.6721	0.4227	0.0336	0.0016	6.1390e-05	2.2663e-05	1.3508e-05
0.95	0.5	1.6811	0.4569	0.0333	0.0012	4.4467e-05	1.7797e-05	1.0647e-05

AIMS Press